RAM ROBOTICS AND MECHATRONICS

DEVELOPMENT OF A SILICONE 3D PRINTING PROCESS ENABLING EMBEDDED SENSORS FOR SOFT ROBOTIC APPLICATIONS

S. (Sybren) Kappert

MSC ASSIGNMENT

Committee:
prof. dr. ir. G.J.M. Krijnen
dr. ir. G.J.W. Wolterink
dr. ir. J.C. Vollenbroek

July, 2023

037RaM2023
Robotics and Mechatronics
EEMathCS
University of Twente
P.O. Box 217
7500 AE Enschede
The Netherlands

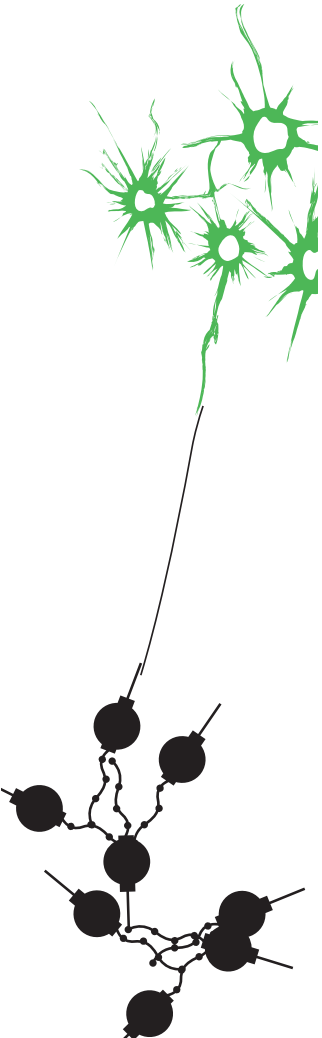

UNIVERSITY OF TWENTE. | TECHMED CENTRE UNIVERSITY OF TWENTE. | DIGITAL SOCIETY INSTITUTE

Summary

Soft robots are inherently safe, adaptive, and tolerant to operating in unknown environments due to the sole use of soft materials. This makes soft robots ideal for applications such as grasping various objects and locomotion over inconsistent terrain. A key concept that currently is being explored to improve the performance and enable the autonomy of soft robots is the addition of sensory feedback. Combining sensing capability with 3D printing has the potential to be a valuable tool for fabricating advanced soft robots. This thesis presents the development of a silicone 3D printing process enabling embedded sensors for soft robotic applications. Materials were selected that meet the challenging demands of soft robots while being compatible with the direct ink writing (DIW) 3D printing process. A conductive silicone composite based on a carbon black filler was developed to enable remarkably soft yet functional sensing structures. The research on this material encompassed processing, characterisation, and 3D printing. Characterisation involved the evaluation of electrical, mechanical, electromechanical and printability properties under various filler concentrations. The findings of this research offer a promising outlook, paving the way for further development of this 3D printing process.

Acknowledgements

I would like to express my gratitude towards the individuals that have played a key role in my thesis. Thanks to their support I have had an enjoyable and rewarding experience over the past year.

First of all, I would like to thank my supervisor Professor Gijs Krijnen for giving me the opportunity to continue my adventure at the NIFTy research group with this thesis.

I would like to thank my daily supervisor Gerjan Wolterink for supervising me in this research subject that was new to both of us.

The guidance by Gijs en Gerjan has allowed me to develop my personal and professional skills. Their unwavering support has ensured that I remained passionate about my research, despite some challenges that arose. I also want to thank them for the opportunity to participate in three research-related activities which included the Dutch Soft Robotics Symposium, Formnext Expo and Silicone Expo Europe.

I would like to thank the other members of the NIFTy research group including Alexander Dijkshoorn, Dimitris Kosmas, Heime Jonkers, Riccardo Sneep and Remco Sanders for their critical eye and tolerance of my sometimes overextended presentations during the biweekly meetings.

Lastly, I would like to thank RaM students Wouter Kockelkoren and Ruben Ufkes for the interesting conversations and exchange of ideas.

Contents

List of acronyms

FDM	Fused Deposition Modeling
DIW	Direct Ink Writing
SLS	Selective laser sintering
SLA	Stereolithography
TPU	Thermosplastic Polyurethane
PDMS	Polydimethylsiloxane
MEMS	Microelectromechanical systems
CB	Carbon black
GNP	Graphene nanoplatelet
CNT	Carbon nanotubes
AgNP	Silver nanoparticle
CuNP	Copper nanoparticle
NIFTy	Nature Inspired Fabrication and Transduction, research group

1 Introduction

1.1 Context

Conventional 'hard' robots use rigid actuated joints for movement. This is beneficial for applications that require high precision, speed, and repeatability such as industrial automation. However, this rigidity poses a challenge when the robot experiences contact with its environment. Advanced control strategies using sensors are necessary to ensure safety and performance while tolerance to unknown environments is very limited. Soft robots instead are inherently safe, adaptive, and tolerant to operating in unknown environments due to the sole use of soft materials [1]. This makes soft robots ideal for applications such as grasping various objects [2] and locomotion over inconsistent terrain [3]. Soft robotics is a rapidly growing field that has emerged over the past decade [4]. A key concept that is being explored to improve performance and enable autonomy is the addition of sensory feedback. Proprioception (the sense of shape and position) and tactile sensing (the sense of contact) are necessary to understand deformations of both internal and external origin [5]. The addition of sensing capabilities is a step towards intelligent soft robots. Advances in additive manufacturing have enabled 3D printing of soft materials. 3D printing of soft robot actuators has the potential to be a valuable tool to fabricate functional complex soft robots [6]. Especially interesting is the use of multi-material printing to enable the fabrication of embedded sensor structures.

1.2 Problem statement

Whereas soft robot sensing research was declared at a state of infancy in 2018 [5], an extensive scientometric review of soft robots showed sensing as being of particular research interest in 2022 [7]. This review stated three emerging trends: new materials, 3D or 4D printing, and sensing and intelligence. The former includes the development of conductive materials for sensing applications. These findings clearly show the current relevance of this topic. Combining soft robot sensing with 3D printing fits perfectly within the current trends. Interestingly, only limited research efforts have been made to combine these features.

Developing state-of-the-art 3D printed soft robot actuators with embedded sensors requires a novel method of fabrication. The current challenge, therefore, is in the development of a 3D printing process that makes use of the latest developments in the fields of 3D printing, materials, and soft sensors. A powerful tool for soft robotics research becomes available once this is achieved.

Most 3D printers use the fused filament fabrication (FFF) technique. This process uses a heated nozzle and is typically limited to thermoplastic materials. Flexible materials are commercially available in the form of thermoplastic polyurethanes (TPU) but these materials have limited stretchability [8]. An alternative technique, direct ink writing (DIW), uses liquid inks instead of thermoplastic materials. This method enables the use of materials with superior properties for soft robotic applications such as silicone elastomers and hydrogels [6]. It is a versatile method that maintains multi-material capability. Systems implementing this technology have only recently surfaced on the market [9, 10, 11]. Due to the recency of these systems and the immaturity of research on printable materials, few attempts have been made at 3D printing soft robots with embedded sensors using this technique. Research on suitable materials and subsequent printing of these materials for the purpose of soft robots is necessary.

Materials research will need to cover both structural materials of the base structure and conductive materials for the sensor structures. In addition to having favourable properties for soft robotics, the materials must be easy to synthesise, have low toxicity, and must be suitable for DIW 3D printing. The conductive material must meet similar mechanical requirements to the

structural material to not impede the mechanical performance of the actuator and should survive the high-strain nature of soft robotic applications [6]. The combination of high stretchability and good conductivity is a challenge that always involves a trade-off [5]. Materials that comply with these criteria are to be developed and analysed to evaluate their fitness for the application of 3D printed soft robot actuators with embedded sensors. Development of these materials is expected to be challenging due to the demanding criteria, immaturity of developments in the research field and initial deficiency in knowledge of polymer science and processing within the research group.

1.3 Related work

Relevant literature can be found in the fields of pneumatic actuators, 3D-printed soft robot actuators and 3D-printed soft sensors. These fields are explored separately as well as attempts that have been made at combining these.

1.3.1 Soft pneumatic actuators

Various means of actuation are possible in soft actuators for soft robotic applications. Examples include pressure-driven, explosive, photo-responsive, magnetically responsive and electrically responsive stimulation [12]. Pressure-driven stimulation is commonly used on larger actuators such as grippers [4], whereas thermal stimulation and electrical stimulation are commonly used in microelectromechanical systems (MEMS) [12]. This research focuses on pneumatic actuators, a class of pressure-driven actuators. These actuators are commonly referred to as pneu-nets.

Soft pneumatic actuators achieve movement by inflating chambers with air. These chambers are designed such that the actuator follows a desired motion, typically a bending motion. The pneu-net actuator was introduced by the Whitesides Research Group at Harvard. Early examples shown using this design were a gripper [13] (Figure 1.1a) and locomotive robot [3] (Figure 1.1b). The design was improved within the research group several years later [14] (Figure 1.1c). This design has been a source of inspiration for soft pneumatic bending actuators ever since. Pneu-net actuators are typically fabricated by casting soft silicone elastomers into moulds.

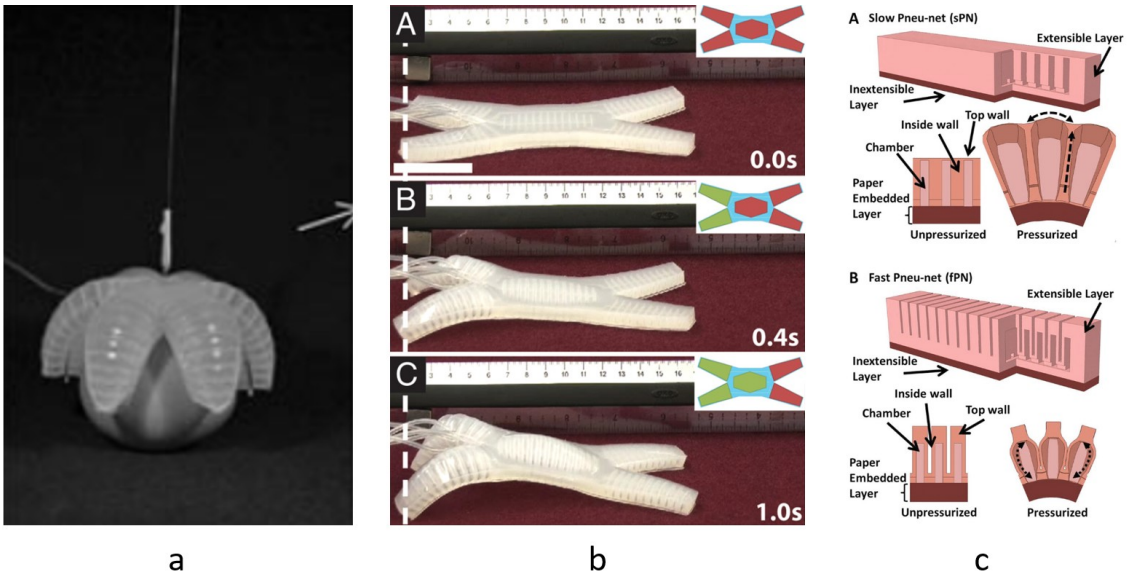

Figure 1.1: The pneu-net and its applications. (**a**) A soft gripper [13]. (**b**) A locomotive robot [3]. (**c**) The improved pneu-net design [14]

.

1.3.2 3D printed soft robot actuators

The challenge in 3D printing soft actuators is in developing fabrication strategies that allow the use of materials that enable functional and safe soft robotics. Wallin et al. extensively studied materials and techniques to fabricate soft robotic actuators using 3D printing [6]. Essential mechanical material properties for soft robots were determined to be a low elastic modulus, a high ultimate elongation, a high toughness and a high modulus of resilience. This is necessary for fabricating soft, elastic soft robots. At the same time, these materials should be printable. This means that the materials can be extruded and that they are able to retain their extruded shape in their mobile state (when molten, in powder form, or prior to curing). Only three 3D printable materials have been identified that have suitable characteristics for soft robotics. These are polyurethanes, silicones and hydrogels [6].

Polyurethanes can be 3D printed using various methods including fused filament fabrication (FFF), selective laser sintering (SLS), and direct ink writing (DIW). Thermoplastic polyurethanes (TPU) have been used in FFF printing to produce soft actuators [15, 16, 17]. An example is shown in Figure 1.2a. Rob Scharff et al. developed a hand consisting of soft actuators using SLS printing with TPU [18]. While some examples with TPUs have been shown, this material is limited in its use for pneumatic soft actuators as it achieves relatively little deformation compared to alternatives due to its higher stiffness [19].

Silicone elastomers, more specifically polydimethylsiloxanes (PDMS), are commonly used for soft robotics [6]. Printing techniques that are compatible with this material are DIW, stereolithography (SLA) and inkjet printing. Silicones exhibit improved material properties over polyurethanes including lower elastic hysteresis [20]. They can be incredibly flexible while offering good temperature stability, electrical insulation and biocompatibility. Due to their high performance, silicone elastomers are widely used in industrial applications ranging from aerospace to medical applications [21]. A large contribution to research on 3D-printed silicone soft robotics is being made by Jennifer A. Lewis et al. Their research includes a multi-material DIW 3D printing technique, named embedded 3D (EMB3D), which has been applied to soft sensors and soft robotics [22, 23, 24]. Other researchers developed a DIW 3D printing system and used it to print a pneumatic soft actuator [25]. This actuator is shown in Figure 1.2b. The performance of this actuator matched a moulded counterpart. A similar approach was shown by J. Li et al. [26]. In addition to DIW, inkjet printing has been demonstrated as a technique to fabricate pneumatic soft actuators [27].

Hydrogels consist of polymers and a high water content. These polymers crosslink into networks which swell due to water absorption [28]. The degree of swelling can be made sensitive to specific stimuli such as temperature and light. Hydrogels are generally biocompatible and are thus often used for biomedical applications. Hydrogels seem to be a promising soft robotics material but are currently not suitable for real-world applications as they often require protection, rehydration and a controlled environment to maintain stable [6]. Improvements are made in this regard but the application of hydrogels is still limited due to their poor mechanical strength [28]. An additional obstacle is that the synthesis of hydrogels for these applications requires advanced chemical processing. 3D printing of modified hydrogels is possible with DIW and SLA techniques. Photopolymerizable hydrogels for SLA printing have been demonstrated [29]. The sensitivity to stimuli is commonly used as actuation method in hydrogels. Few attempts have been made at hydraulically and pneumatically driven actuation [30]. A DIW 3D-printed hydrogel fluidic soft actuator was achieved by developing a rheology-modified hydrogel with enhanced strength and toughness [31]. This actuator is shown in Figure 1.2c.

1.3.3 3D printed soft strain sensors for soft robotic applications

Sensors can be used to detect or measure desired physical parameters of a system. Parameters particularly interesting for soft robotics are its state of deformation and applied contact force.

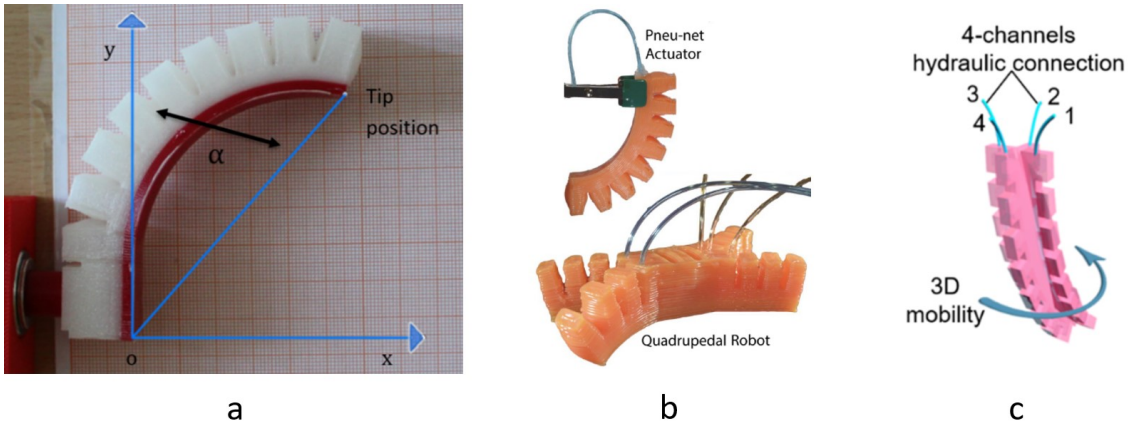

Figure 1.2: Fluidic soft actuators fabricated using 3D printing. (**a**) A FFF printed pneumatic actuator made from thermoplastic polyurethane [15]. (**b**) A DIW printed pneumatic actuator made from a silicone elastomer [25]. (**c**) A DIW printed hydraulic actuator made from an elastic hydrogel [31].

.

Changes in deformation are measured using strain sensors, often referred to as strain gauges. Typical strain gauges are made from metals and are optimized for small strains. These sensors are unsuitable for soft robotics as they lack compliance to operate under the high-strain conditions experienced by soft robots [32]. Instead, strain sensors fabricated using soft materials are being considered.

Common strain sensors include resistive and capacitive sensors. Resistive strain sensors function by measuring their resistance under strain. The resistance is affected by the Poisson effect and the piezoresistive effect. The Poisson effect is a geometric effect that describes the tendency of a material to contract in the direction transverse to the axial direction of stretching. The ratio of negative transverse strain to axial strain is known as Poisson's ratio. This number is generally between 0 and 0.5, where soft materials tend to be close to 0.5. The response of a strain sensor is typically described by its gauge factor which is the ratio of relative change in resistance $\frac{\Delta R}{R}$ to strain ϵ.

$$\nu = -\frac{\Delta\epsilon_{\text{transverse}}}{\Delta\epsilon_{\text{axial}}} \tag{1.1}$$

$$GF = \frac{\frac{\Delta R}{R}}{\epsilon} \tag{1.2}$$

The relative change in resistance based on the geometric effect is [33]:

$$\frac{\Delta R}{R} = (1+2\nu)\,\epsilon \tag{1.3}$$

Given a Poisson ratio of 0.5, the expected gauge factor would thus be 2. This equation assumes the electrical resistivity to be constant. However, this is generally not true. The strain-dependent resistivity contribution is described by the piezoresistive effect. When including this effect, the relative change in resistance becomes [33]:

$$\frac{\Delta R}{R} = (1+2\nu)\,\epsilon + \left(\frac{\Delta\rho}{\rho}\right)_l \epsilon_l + \left(\frac{\Delta\rho}{\rho}\right)_t \epsilon_t \tag{1.4}$$

where $\left(\frac{\Delta\rho}{\rho}\right)_l$ and $\left(\frac{\Delta\rho}{\rho}\right)_t$ are the changes in resistivity due to longitudinal and transverse strain.

Capacitive strain sensors function by measuring the change in capacitance under strain. They consist of (at least) two electrodes with a dielectric in between. An applied strain typically changes the distance between these electrodes causing a change in capacitance. Capacitive

sensors generally show lower hysteresis and higher sensitivity [32]. The capacitance is only dependent on the distance and overlap of the electrodes. The sensor is thus not affected by the nonlinear effects due to the resistivity seen in resistive sensors. However, capacitive sensors require shielding as they are sensitive to parasitic capacitances [34]. Capacitive sensors add complexity and may not be a viable option in all designs. Resistive sensors are easier to implement and the nonlinearities can be improved using compensation methods [35]. Capacitive sensor designs can be considered when higher linearity is required.

A necessity shared by both resistive and capacitive strain sensors is the need for a conductive material. In soft robotics, this material should meet similar mechanical requirements as the structural material used for the soft actuator. Four types of conductive materials have been shown to be suitable for this application. These are liquid conductors, conductive inks, and conductive elastomer composites. Each of these is also compatible with DIW 3D printing. Three examples are shown in figure 1.3.

Common liquid conductors are liquid metals and ionic liquids. These liquids are injected into predetermined channels in situ or post-print. The shape of these channels and subsequently the liquid that it contains changes due to the geometric effect. Examples devoted to soft robots include a saltwater-based sensor [36] and various sensors based on gallium-based alloys such as EGaIn and galinstan [37]. The hysteresis of liquid conductor sensors is good due to the absence of the piezoresistive effect. However, the fabrication of leak-free microchannels is challenging with 3D printing methods. Design freedom is limited as liquids can not be used to fabricate self-supporting 3D structures and surface layers. Liquid metals show excellent resistivity but have a limited temperature working range due to their melting temperature (e.g. EGaIn 15.5 °C) and toxicity concerns remain despite the introduction of low-toxicity galium alloys. Liquid metals can influence the behaviour of soft sensors due to their relatively high density. Ionic liquids have a lower density but show poor resistivity, large temperature drift, and poor stability due to electrolysis [5].

Conductive inks are a suspension of conductive nanoparticles, typically metallic nanoparticles, in solvents. After deposition, the solvents evaporate resulting in a thin conductive film [38]. This method is commonly used for 3D printing electronics due to the material's low resistivity [39]. Flexible silver-based inks are being researched [40], but these materials are still too stiff and are prone to cracking under small strains. Furthermore, embedment of sensors is difficult due to the required solvent evaporation and the fabrication of 3D structures is unattainable due to the thin layers. Silver-based ink has been shown in a soft robot sensor but the sensor was located near the neutral line where strains are small [41]. This soft actuator was assembled in parts presumably to allow for solvent evaporation during fabrication.

Conductive elastomer composites are piezoresistive materials that consist of an elastomeric matrix with a conductive filler. Silicones and urethanes are examples of suitable highly flexible elastomers. Materials with equal or similar mechanical properties to the soft actuator's structural material can thus be selected. Choosing the same material for both also provides good adhesion between these materials. Examples of conductive particle fillers are silver nanoparticles, carbon blacks and carbon nanotubes. An elastomer composite is the only material of three that can be used to fabricate self-supporting 3D structures and is thus the only 'real' 3D-printable conductive material. Mechanical and electrical properties can be tuned by altering the type of elastomer and filler content. The primary disadvantage of using this material as a sensor is the large hysteresis and nonlinearity due to the piezoresistive effect. Yet, this type of material has been widely used for sensors in soft robots [5]. These composites have a relatively high resistivity but this is not a problem in most sensing applications.

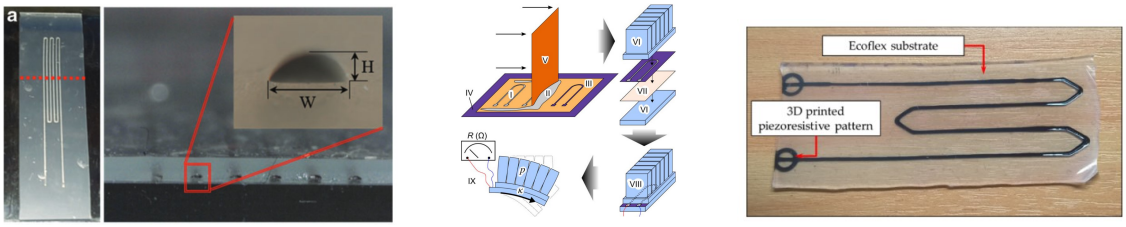

Figure 1.3: (**left**) A DIW 3D printed EGaIn liquid conductor strain sensor [42]. (**centre**) A screen-printed silver ink strain sensor [41]. (**right**) A DIW 3D printed silicone elastomer carbon black composite strain sensor [43].

Table 1.1: Characteristics of conductive materials for soft robot sensors

Type	subtype	Stretchability	Design freedom	Resistivity	Hysteresis/Linearity	Stability
Liquid conductor	liquid metal	++	-	++	++	+
	ionic liquid	++	-	-	++	- -
Conductive inks		- -	- -	+	+	+
Elastomer composite		+	++	-	-	+

1.3.4 3D printed soft robot actuators with embedded sensors

As research advancements in the fields of 3D-printed soft actuators and 3D printed soft sensors continue, it becomes increasingly interesting to explore their integration. Co-fabrication of structural and conductive materials enables the embedment of sensor structures. These sensor structures are not limited to application on surfaces of the actuator as conventional sensors would. This unlocks new possibilities such as three-dimensional structures to measure areas of interest within the soft actuator and enable multilayer capacitive structures.

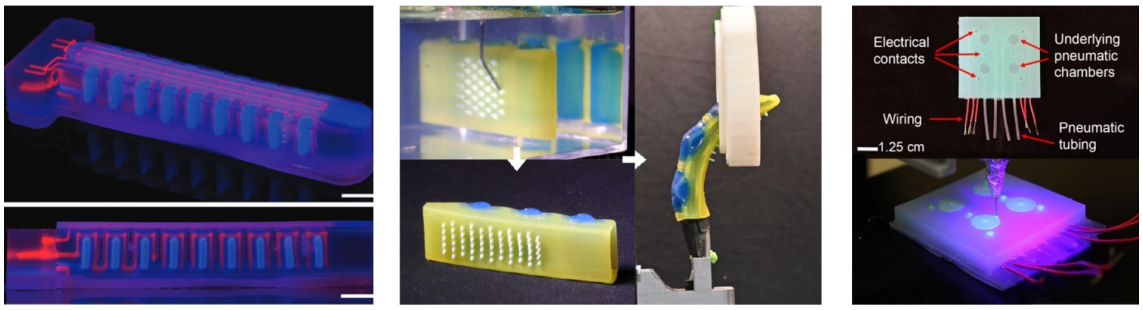

Figure 1.4: Fluidic soft actuators with embedded sensors fabricated using 3D printing. (**a**) A silicone actuator with multiple ion gel resistive strain sensors fabricated using the DIW-based EMB3D technique [23]. (**b**) A silicone actuator with a carbon grease-based resistive strain sensor fabricated using the DIW-based FL-3DP technique [44]. (**c**) A photopolymerizable silicone actuator with conductive hydrogel capacitive tactile sensors fabricated using multimaterial DIW printing [45].

Interestingly, only a few attempts have been made at fully 3D printing soft actuators with embedded sensors. The most notable contribution was made by Truby et al. using the aforementioned custom DIW-based multi-material EMB3D printing process [23]. This is an advanced pneumatic soft actuator with embedded curvature, contact, and inflation sensors (see Figure 1.4a). The latter features a three-dimensional structure. Three different silicone elastomers with a durometer ranging from a Shore 00 hardness of 10 to a Shore A hardness of 40 were used as structural anterior, actuator and dorsal matrices. These materials do not possess the required rheological properties to be 3D printed using conventional methods. Layer-by-layer

formation with these materials is not possible as they are unable to retain their extruded shape after deposition, let alone support their shape under the influence of subsequent layers. Instead, the presented method uses these materials as supporting baths shaped using a three-step moulding process. The resistive strain sensors and inflation bladders are then structured within these supporting baths using 3D printing. The soft actuator is thus not fully 3D printed, only its embedded structures are. The multi-step fabrication requiring moulds diminishes the benefits of flexibility promoted by 3D printing. Additional processing steps are necessary to evaporate the required volatile ink to create air bladders for actuation. An ion gel liquid conductor was developed to function as the sensor material. This material is soft enough not to interfere with the actuator's movement and shows low hysteresis but suffers from the aforementioned poor stability.

A similar 3D printing process named freeform liquid three-dimensional printing (FL-3DP) was developed by Calais et al. [44]. The support bath in this method has a different purpose. It solely acts as a support in which the structural and conductive materials are printed. At first glance, this seems an ideal solution to enable both fully 3D printed structures and the use of materials otherwise not printable with traditional techniques. However, this technique is plagued by difficulties in controlling the interface between the printing materials and support bath material. This research showed that sufficient control can be achieved through an in-depth study of the materials' rheological properties. Balancing governing rheological properties between the materials was critical for successful printing. A functional pneumatic soft actuator was fabricated using two types of silicone and a carbon grease-based sensor material (see figure 1.4b). Characterisation of the sensor was limited as it was primarily used for demonstrative purposes. The FL-3DP method is a promising alternative to traditional silicone printing techniques by enabling the use of otherwise incompatible materials at the expense of requiring an in-depth understanding of the rheological properties of these materials.

Methods employing more traditional techniques to produce 3D printed silicone soft actuators like those shown in section 1.3.2 have been expanded with the ability to print embedded sensors. Robinson et al demonstrated a method using a rheology-optimised photopolymerizable silicone blend as structural material and an ionically conductive hydrogel to create capacitive sensor structures [45]. In situ photopolymerization allows the structural material to fix its shape after extrusion. A pneumatically actuated haptic device with tactile sensors was fabricated using this technique (see Figure 1.4c). Other examples of 3D printing pneumatic soft actuators with embedded sensors have shown mixed results. As an example, Shih et al. used a commercial inkjet 3D printer with proprietary materials [46].

The challenges in these studies clearly stand out from the 3D-printed soft actuator and soft sensor research seen before. Those studies focus on the synthesis and characterisation of advanced materials to improve actuators and sensors but lack consideration of the implications of combining them. The studies shown here aim to tackle this by developing 3D printing processes that consider the interaction of materials, multi-material printing techniques, and requirements for soft robotic applications but fall short in motivation and analysis of the sensor material. The sensor is generally perceived as an attractive feature rather than an essential part of the entirety. Analysis of the electrical and electromechanical properties and their implications for sensor designs in soft actuators is either rudimentary or nonexistent.

1.4 Project goal

Relevant literature has revealed interesting research opportunities. In order to facilitate advancements in soft actuators, new approaches to 3D printing processes should be investigated. The goal of this thesis is therefore to develop a novel 3D printing process for soft robotic actuators with embedded sensors. This 3D printing process aims to combine knowledge and

methods of the different fields to promote embedded sensors with improved characteristics and design flexibility in soft robotic applications.

The to-be-developed 3D printing process aims to tackle the deficiencies found in current methods. The following features should be integrated into the 3D printing process in order to surpass current methods.

- **Fully 3D printable actuators:** No in-situ processing steps such as partial mould casting should be necessary. The 3D printing process should fully utilize the flexibility offered by 3D printing.
- **Large sensor design freedom:** The 3D printing process should allow the fabrication of conductive self-supporting structures to enable complex three-dimensional embedded and superficial sensors. This makes it functional for a wide range of applications.
- **Novice level processing:** The importance of processing difficulty is often disregarded in research despite being crucial in making methods accessible. Advanced materials often require extensive processing steps and the use of possibly hazardous materials such as solvents. The methods of material processing are frequently undescribed making results unapplicable to novices or even unreproducible due to the lack of information. The aim of this 3D printing process is to keep processing complexity to a minimum. The proposed materials should be processable by those interested in printing soft actuator designs but who have limited knowledge of materials and processing. Achieving this would make the developed process applicable to a wider range of researchers including those focused on applied research.
- **Comprehensive characterisation of the conductive material:** The conductive material used for the sensor structures should be perceived as an integral part. The characteristics of this material highly influence its applicability to future designs. Therefore, analysis of the material with respect to its use in soft robots should be investigated. Characterisation of the electrical, mechanical, electromechanical and printability properties gives insight into its fitness for this application. This information can be used to select formulations with desired characteristics for specific applications in future work.

By combining the problem statement with the findings from the literature review the following research question can be formulated:

> *What should a 3D printing process, that enables embedded sensing for soft robotic applications, look like?*

Development of a 3D printing process requires the selection, processing, characterisation and printing of suitable structural and conductive materials. To support these aspects, three research sub-questions have been formulated. In order, these are sub-questions related to the selection, processing and characterisation of materials:

> *Which structural and conductive materials comply with the demanding criteria of soft robotics while being compatible with the used DIW 3D printer?*

> *How can the selected materials be processed successfully using a method with minimal complexity?*

> *How does the formulation of the developed conductive material affect the mechanical, electrical, electromechanical and printability properties?*

1.5 Approach

The development of a new 3D printing process including materials requires a multidisciplinary approach. It is not possible to address all aspects within the timespan of this thesis. A MoSCoW prioritization of the tasks to be addressed in this thesis can be found in Appendix A. This thesis will include research on both structural and conductive materials but the focus is on the latter. The approach of this thesis can be separated into four steps that aim to give answers to the research (sub-)questions.

1. **Material selection:** Criteria and desired characteristics for the materials in the 3D printing process should be determined. These include electrical, mechanical, processing and printability traits. Challenges in applying these materials are to be identified. Literature is to be utilised to support this and identify potential solutions. Suitable products for the structural and conductive material are to be selected.

2. **Material processing:** A reproducible processing method with minimal complexity is to be developed. This includes both synthesis and subsequent curing tactics for the materials. The effect of processing techniques and parameters on the properties of the conductive material is to be studied.

3. **Material characterisation:** The materials are to be characterised in terms of the electrical, mechanical, electromechanical and printability properties. The impact of alterations in the conductive material's formulation on these properties is to be studied. This should also give insight into the limitations of this material.

4. **Additive manufacturing:** Reliable methods for printing both materials individually using the DIW 3D printer are to be determined. This includes the selection of appropriate tools with accessories and parameter tuning. Models are to be printed to test the capabilities of the materials and printing process and identify challenges.

1.6 Report structure

This introduction chapter has discussed the context, problem statement and literature related to this research to motivate this thesis' goal and approach. The core chapters are based on four steps discussed in the approach. Material selection is dicussed in chapter 2, material processing in chapter 3, material characterisation in chapter 4, and additive manufacturing in chapter 5. The conclusions and future recommendations of this thesis can be found in Chapter 6.

2 Material selection

2.1 Introduction

A Brinter 3D printer based on the direct ink writing (DIW) technique will be used in this thesis. Materials compatible with this printer that have favourable characteristics for soft actuators with sensors are to be selected. Various materials suitable for this application were discussed in the introduction's related work section. Based on the findings of this study and by considering the desired features of this 3D printing process, silicones are chosen to be the structural material type and conductive silicone composites are chosen to be the conductive material type. Silicones exhibit proven favourable characteristics associated with soft robotic applications compared to urethanes and hydrogels while being commercially available and requiring minimal processing complexity. Conductive elastomer composites are the only materials that can be designed to allow the fabrication of complex self-supporting sensing structures both in embedded form and at the surface, which is one of the desired features of the 3D printing process. Excellent stretchability and adhesion to the structural material are ensured by choosing a silicone elastomer base. The poor hysteresis and linearity seen in these materials can potentially be improved in the future using compensation methods [35]. These methods are similar to those involving conductive thermoplastic urethane sensors currently studied by the NIFTy research group. The mechanical and electrical properties of this conductive material can be tuned by altering the filler content and silicone matrix. This research will focus on resistive strain sensing because of its reduced complexity and greater design freedom compared to capacitive sensing. In case improved hysteresis and linearity are desired in the future, capacitive sensing can be applied without altering the material.

To explore potential solutions for the structural and conductive material and identify challenges, this chapter includes a literature study. Desired characteristics for these materials in the 3D printing process are determined. Available products for the materials are selected based on these characteristics.

2.1.1 The Brinter One DIW 3D printer

A 3D printer was acquired for this soft robotics project. This is the Brinter One, a printing platform primarily developed for bioprinting [9]. The platform has support for multiple tools that cover the majority of the materials spectrum. This includes multiple tools suitable for DIW printing of silicones. Tools available during this thesis were the Visco Tool and the Pneuma Tool Heated/UV (see Figure 2.1a and 2.1b). The Visco Tool is a screw extruder that can handle high viscosity inks. This tool allows direct control over material flow with high precision including the possibility to do retractions. The screw extrusion technique allows it to control flow independent of material viscosity. A downside of the Visco Tool is that fast curing inks can cure inside the extrusion system which requires disassembly of the system. Changing inks requires bleeding and possibly disassembly. The Visco Tool is a pneumatic extruder that uses disposable syringes. Changing materials is easy and there is no risk of damaging the system with fast curing inks or contamination from previously used materials. The downside of using this tool is that control over the extrusion is limited. Materials with different viscosities and different tips require different pressures to obtain desired extrusion. Calibrations will fail in case the pressure requirement changes during printing. The operating principles of pneumatic extrusion and screw extrusion are shown in Figure 2.1d. The Pneuma Tool has a built-in UV LED light for use with UV-curable inks. In addition to this, a LED module with UV LED has been installed on the tool changer. This enables the use of UV-curable inks with other tools such as the Visco Tool. The printer can operate up to four tools for multi-material printing.

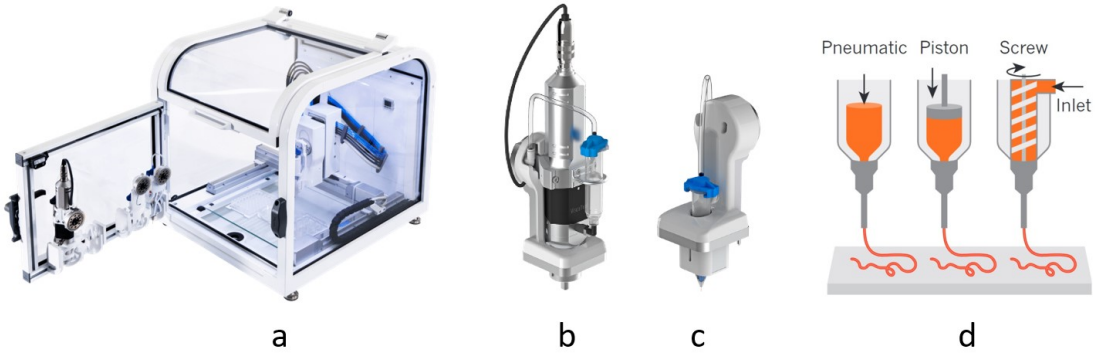

Figure 2.1: (a) Brinter One Bioprinter **(b)** Visco Tool **(c)** Pneuma Tool Heated/UV **(d)** DIW printing techniques [47].

2.2 Related work

2.2.1 3D printable silicones in research

DIW 3D printing of silicones is fundamentally different from FFF 3D printing TPUs. TPUs are thermoplastic materials of which a reversible molten state can be achieved by heating. The material is extruded in its molten state. After deposition, the material cools down and its extruded shape is fixed. This makes layer-by-layer object formation possible. Silicone rubber is a thermoset material. The printability of this material is rheology dependent rather than temperature dependent [48]. They have an uncured and a cured state which are not reversible. In their uncured state, silicones are liquid. The curing of silicones is a chemical process that can be obtained in various ways. Two common silicone systems are addition cure systems and condensation cure systems. Addition cure systems, typically platinum-catalysed, offer a fast curing rate for with no byproducts. This makes them ideal for medical (skin-safe) and food applications. Activation of the platinum catalyst and acceleration of the curing is commonly achieved with heat. Although it is possible to initiate curing at room temperature. Platinum-catalysed systems consist of two components. The reaction is initiated directly after mixing these components. Alternatively, photoactive catalysts can be used to initiate curing under the influence of light [49]. This allows for fast curing characteristics when heat induction is not possible. Addition cure systems can be sensitive to cure inhibition due to incompatible materials. The alternative to addition cure systems are condensation cure systems, which are generally tin-catalyzed. Condensation cure systems cure when exposed to ambient moisture. These silicones can be found in both 1-component and 2-component variants that work using different principles. Their rate of curing cannot be accelerated using heat and the reaction produces byproducts. They exhibit worse mechanical properties compared to addition cure systems and suffer from shrinkage which should be taken into account with fabrication.

Silicones of both addition and condensation systems have been applied in 3D printing. The rheological properties of plain silicone do not allow 3D printing. The material is not able to retain its shape after deposition for a sufficient duration to transition into the cured state. The rheological behaviour most influential on the printability is shear thinning, or more specifically the yield stress character [6, 50, 51]. Shear thinning is the behaviour where the viscosity of fluids decreases under shear strain. Yield stress is the maximum stress at which the material elastically deforms. Higher stresses cause plastic deformation, in this case meaning the material's failure to retain its extruded shape. Shape retention can be achieved with sufficiently high yield stress. Higher viscosity silicones show higher yield stress but this is generally insufficient. Instead, rheology modifiers such as (nano-)silica [52] and fibres [53] are used to improve printability by increasing the yield stress. Optimal rheological properties can be obtained by tuning

the amount of silica [50]. However, it should be noted that these modifiers also affect the mechanical properties of the cured material [54]. The shape retention capability of silicones in their uncured state can be studied by measuring their elastic modulus and viscous modulus under shear stress [45]. Curing of silicones can be slowed by inhibitors such that rheological properties remain more constant during printing.

2.2.2 3D printable silicones in industry

Commercial 3D printers implementing silicone 3D printing have surfaced in recent years. Lynxter has released their S600D printer with tools for either 1-component or 2-component silicone systems [11]. Both systems use progressive cavity extruders. The 2-component tool uses a static mixer. Room temperature vulcanization silicones modified for 3D printing are used. A newer model, the S300X, implements one 2-component tool and one 1-component tool that allows multi-material printing. The 1-component tool is generally used with a water-soluble support material. Unfortunately, the materials used in these systems are proprietary. Delta Tower has a similar approach with their Fluid ST printer [10]. This system can be configured with up to six tools, including tools for 1-component and 2-component silicones. This allows true multi-material silicone printing. Their silicone materials are developed by the company Elkem. Elkem's AMSil^{TM} line of materials is composed of 1-component and 2-component condensation cure silicones and a water-soluble support material tailored for use by 3D printing [55]. These products are commercially available outside Delta Tower's product line. The performance of these materials has been studied using traditional [56, 57] and support bath [58] methods (see figure 2.2a).

The printer used in this thesis, the Brinter ONE, has also been demonstrated with silicone printing [9]. Both the Pneuma Tool and the Visco Tool can be used to print silicones. However, it should be noted that these tools do not include dual extruders with static mixers typically required for 2-component systems. The choice of silicones is thus limited. Brinter recommends Momentive Silopren^{TM} UV LSR 2030, a commercially available photocatalyzed (likely platinum-based [49]) silicone, for 3D printing. The printability and curing characteristics of this material have been studied [59, 60] (see figure 2.2b).

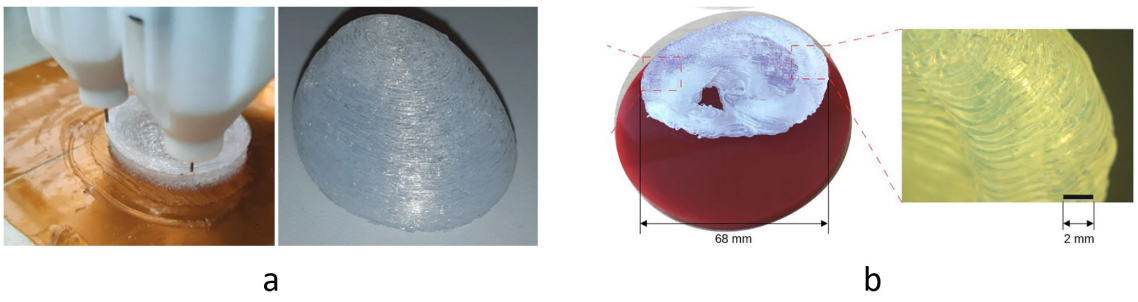

Figure 2.2: Commercially available 3D printable silicones. (**a**) A thin-walled bladder model 3D printed using Elkem AMSil 20101 condensation cure silicone. [56]. (**b**) An ear model 3D printed using Silopren UV LSR 2030 photocatalysed addition cure silicone [60].

2.2.3 Conductive fillers

Silicone by itself has a high resistivity ranging from $1 \times 10^{14}\,\Omega$cm to $1 \times 10^{16}\,\Omega$cm making it a good insulator. Conductive silicone rubbers can be achieved by creating a conductive silicone composite using conductive fillers. Options are carbon-based fillers and metallic fillers that yield a composite resistivity in the range of $1\,\Omega$cm to $1000\,\Omega$cm [21]. Carbon-based fillers include carbon black (CB), carbon nanotubes (CNT), and graphene nanoplatelets (GNP). Metallic fillers comprise mainly of silver nanoparticles (AgNP). The particle size of these fillers in the composite is sufficiently small to prevent nozzle clogging during the printing process. Con-

ductivity is achieved through conductive networks created by the filler's particles. The relation between resistivity and filler content is not linear. Conduction of electricity is only possible if there is a sufficiently developed conductive network. The filler weight fraction at which this occurs is called the percolation threshold [61]. The resistivity rapidly decreases at this point. This behaviour is explained by percolation theory. A typical percolation curve is shown in figure 2.3.

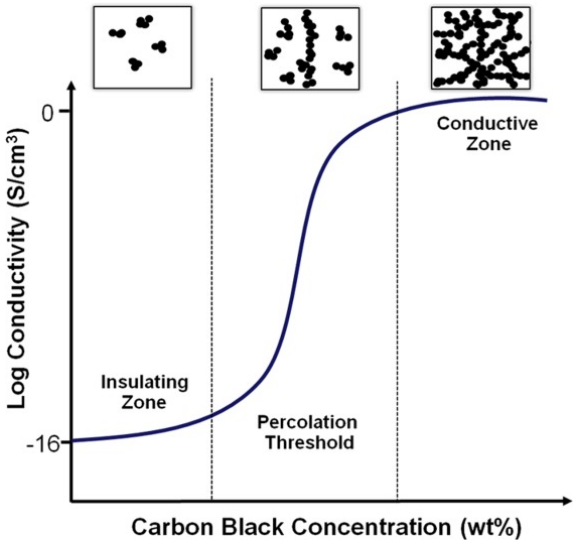

Figure 2.3: A typical percolation curve with percolation threshold [62]

Conductive silicone composites have been studied extensively. This includes research on materials for traditionally fabricated sensors and 3D printed sensors. Carbon black (CB) is the most common conductive filler [63]. This type of filler is commonly used in industry for applications including pigmentation and reinforcement of natural rubbers. However, the type of CB used for these applications is not optimized for conductivity. High filler content is necessary to achieve decent resistivity [64] which negatively affects mechanical properties of the elastomer composite such as stress relaxation [65]. Therefore, specialised highly conductive CB fillers have been developed that reduce the required filler content. These have enabled the synthesis of conductive silicone/CB composites with good mechanical and electrical properties for sensing applications [66]. Interestingly, the addition of CB filler causes favourable rheological properties for 3D printing such as increased viscosity. Printing of two-dimensional [67] and three-dimensional [68] structures has been shown without requiring rheology modifiers. CNTs have a large aspect ratio and specific surface area which yields excellent mechanical and electrical properties but makes homogeneous dispersion even more difficult than CB [63, 69]. Kumar and al determined CNTs to be the best carbon-based material [65]. However, CNTs have carcinogenic potential which makes their use controversial [70]. Silicone / CNT composites have been used to print two-dimensional [71] and three-dimensional structures [72] without additional rheology modifiers. GNP fillers also obtain improved electrical and mechanical properties compared to CB but are also more difficult to disperse properly [73]. GNP particles have been shown to easily agglomerate resulting in large electrical hysteresis under applied loads [43]. 3D printing of silicone / GNP composites in literature is rare. Metallic fillers are an alternative to carbon-based fillers. AgNP-based silicone composites show lower resistivity [69] compared to CB, but have a higher density and are much more expensive (>€100 compared to <€1 per gram). High filler weight fractions yield remarkably low resistivities of under $1 \times 10^{-3}\,\Omega\,\text{cm}$ [74]. 3D printing of three-dimensional structures has been shown with silicone / AgNP composites [75]. No rheological modifiers were necessary with the high weight fraction used as the viscosity increased sufficiently to facilitate the printing process.

2.2.4 Challenges integrating structural and conductive silicone materials

Particular attention should be given to the selection of structural and conductive material silicone matrix when integrating them together in a 3D printing process. Addition cure systems are susceptible to cure inhibition by contact with condensation cure, making the two materials incompatible [76]. The silicone will not cure in the contaminated areas. Furthermore, the difference in shrinkage between the two systems would cause stresses at the boundary layer.

A second thing to be aware of is conductance stability when using both silicones and conductive silicone composites in a 3D printing process. Tavakoli et al found that conductive silicone composites can suffer from significant loss of conductance over time when in contact with other silicones [64]. The influence of six methods of fabrication on the loss of conductivity was tested. The three different cure orders were: conductive silicone first, both together, and plain silicone first. Each of these three was cured at both 130 °C for 25 min and at room temperature for 48 h. It was found that the resistance was increased by over 350% in 7 h when uncured plain silicone was added on top of cured conductive silicone. This effect was much stronger than the converse method. This is caused by the diffusion of the conductive filler, clearly visible in figure 2.4. The results show that it is crucial to avoid curing conductive silicone prior to plain silicone, that it is in contact with, as much as possible. Ideally, a 3D printing system with both materials would deposit and cure the plain silicone prior to depositing the conductive silicone in a layer. The conductive silicone would thus ideally have a long cure time. For the subsequent layer, the deposited plain silicone would then be cured alone or together with the conductive silicone from the layer prior. Currently, there is insufficient awareness of this conductance stability problem in soft sensor research. Its effect should be considered when choosing materials.

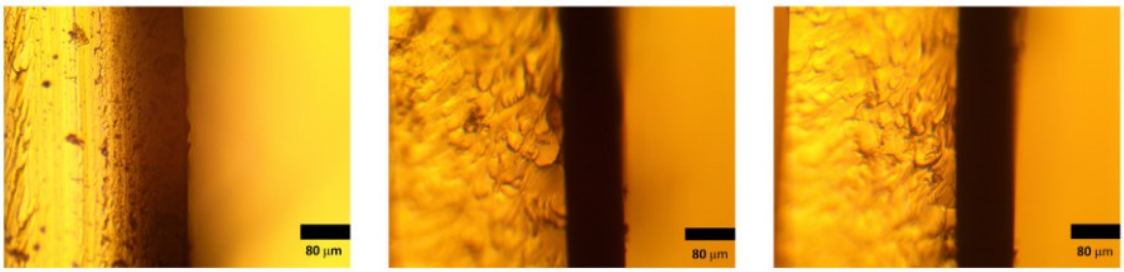

Figure 2.4: Cross-sectional images of plain silicone and conductive silicone cured by different methods **(left)** conductive silicone cured first **(middle)** cured simultaniously **(right)** plain silicone cured first

2.3 Material selection

A structural material and a conductive material are to be chosen for use in the 3D printing process. Desired characteristics for these materials are identified based on the discussed literature. Materials that satisfy these desired characteristics are selected.

2.3.1 Desired characteristics of the materials

Desired characteristics were identified for both materials. This includes a list of shared desired characteristics mainly concerning mechanical and rheological properties. Additional desired characteristics were identified for the conductive material concerning the effects of conductive fillers.

Shared desired characteristics:

S1 **Good mechanical properties for soft robotic applications:** The materials should exhibit suitable mechanical properties. The stiffness of materials is determined by Young's modulus. Recommended values for soft robotic applications are lower than 100 MPa [6]. Soft robotic materials should have an ultimate elongation between 40% and 1000% strain,

where higher is better [6]. Additionally, high toughness and modulus of resilience of the materials are desired [6].

S2 **Good shape retention after deposition** The materials in their uncured state should show sufficient yield stress to have shape retention after being deposited by the 3D printer. The shape retention should be good enough to deposit multiple layers on top of each other with minimal sagging.

S3 **Stable rheological properties before deposition:** The cure dynamics of the material before deposition should be sufficiently slow that rheological properties are not affected during printing. Unstable properties alter the flow behaviour and invalidate calibrations.

S4 **3D printer compatible viscosity:** The viscosity of the materials in their uncured state at the shear stresses experienced during extrusion should not exceed the possibilities of the 3D printer. Deposition of highly viscous materials might not be possible.

S5 **Compatible cure speed:** Bad conductance stability due to conductive filler diffusion was found mainly when depositing uncured plain silicones on cured conductive silicone composites [64]. The cure speed of the structural silicone should be faster than that of the conductive silicone composite to have minimal effect on the conductance stability.

S6 **Minimal processing complexity:** A reproducible processing method with minimal complexity was mentioned as a desired feature of the 3D printing process. Synthesis of the materials should be possible by the NIFTy research group which has little knowledge of material processing currently. Regarding the materials, this means minimal required steps for their synthesis and avoidance of potentially hazardous materials as much as possible.

Conductive silicone composite specific desired characteristics:

C1 **Low silicone matrix viscosity:** The viscosity of conductive silicone composites is known to increase with filler content. To allow for high filler contents while remaining printable, low viscosity of the matrix is desired. Silicone oil can be used to lower viscosity, but volatilizing excessive oil after cure takes a long time [77].

C2 **Low silicone matrix mechanical hysteresis:** The mechanical hysteresis of the matrix influences the performance of sensor structures made from it. Minimal mechanical hysteresis is desired.

C3 **Minimal effect on mechanical properties:** The used filler should minimally affect the mechanical properties of the matrix.

C4 **Wide range of resistivity:** The possibility of altering the filler content for a wider range of resistivity is desired. Low-resistive formulations can be used for long and thin structures. High-resistive formulations can be used to obtain a higher strain sensitivity.

C5 **Good dispersion quality:** A homogeneous dispersion is important for good electrical properties and printability. There is a risk of agglomeration for difficult-to-disperse additives which can cause clogging of the nozzle.

C6 **High gauge factor:** A high gauge factor is desired when using the conductive material for sensitive piezoresistive sensing structures.

2.3.2 Structural material

A silicone elastomer is to be chosen as the structural material. This material be synthesized or a commercially available product could be chosen. The latter was chosen as the development of a suitable formulation would be time intensive with uncertain results. The use of commercially available products also makes the 3D printing process more approachable. Addition cure and Condensation cure systems are considered. The two potential solutions were determined to be the condensation cure based 1-component Elkem AMSil 20101 and addition cure based photocatalysed Momentive Silopren UV LSR 2030. The first cures slowly at room temperature under the influence of ambient moisture, the second cures quickly at room temperature under exposure to 365 nm UV light.

An overview of properties found for both both materials is shown in table 2.1. The desired stiffness/softness of a material was expressed in terms of its Young's modulus. This property could not be found in the technical documents of the material. The reason for this is that Young's modulus is only a good measure for purely elastic materials. Silicone elastomers show viscoelastic behaviour which makes their Young's modulus strain rate dependent. This makes it difficult to compare Young's moduli found in literature. This is especially true when no information on the used strain rate is mentioned as is the case for the two values shown in the table. Producers of silicones prefer to measure the hardness of materials instead. Standardised test equipment, named the Shore durometer, is used. Several Shore scales exist, of which A is most common for elastomers. An overview of the Shore hardness scale is shown in Figure 2.5.

The yield stress of uncured AMSil 20101 was found to be 600 Pa in literature [58]. This value is deemed sufficient as the material has been developed especially for 3D printing. Silopren UV LSR 2030 was not developed specifically for 3D printing but it has shown to be possible [59, 60]. It is the recommended silicone printing material by Brinter [9]. The Brinter recommended method of printing this material does not involve additives. Holländer et al printed without rheology modifiers [59]. However, Fay et al. found that the material shows a higher static storage modulus (G') than loss modulus (G") which indicates liquid-like behaviour before cure initiation [60]. It was found that the rheology could be improved by adding a small amount of thixotropic agent. This increased the viscosity at low shear stresses, which is after the material is deposited. This did not affect the curing behaviour or ultimate elongation of the material. It should be noted that high concentrations of the thixotropic agent can make the viscosity at shear stresses experienced in the extruder too high making deposition impossible.

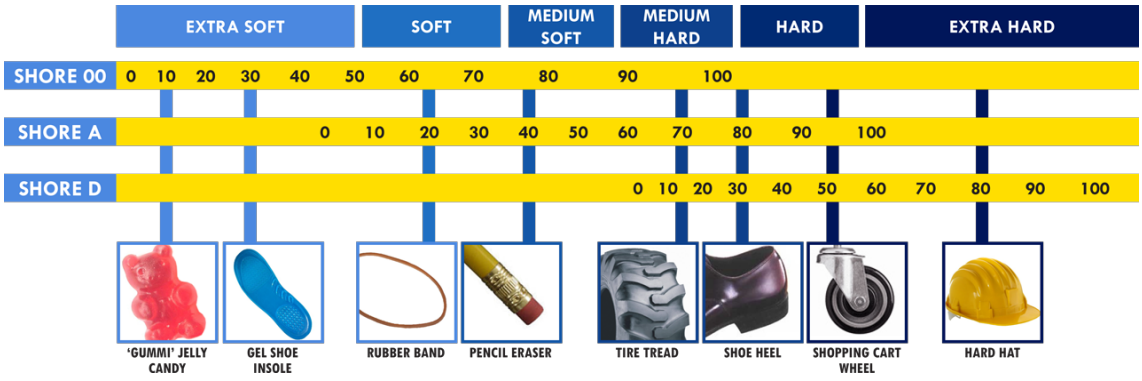

Figure 2.5: Shore hardness scale with exemplary materials [79]

A comparison on the suitability of the two materials is made based on the six desired characteristics discussed earlier. The results are shown in table 2.2. Silopren UV LSR 2030 was shown to be superior to AMSil 20101 for the intended application. Its excellent suitability is primarily due to its unique ability to cure quickly on demand thanks to its photoactive catalysts. Both materials show good shape retention after deposition, but Silopren UV LSR 2030 enables per-

Table 2.1: Silicone / CB composites in literature

Material	AMSil 20101	Silopren UV LSR 2030
Shore hardness	18 Shore A [57]	28 Shore A [78]
Ultimate elongation (% strain)	400 [57] ≈100 (printed) [58]	750 [78]
Young's modulus* (MPa)	≈1 (printed,ISO 527-1) [58]	≈ 0.4 (printed,unknown) [60]
Tensile strength (MPa)	1.1 [57]	8 [78]
Yield stress uncured (Pa)	600 [58]	-
G' uncured (Pa)	-	750 (0%) 15000 (0.05%) [60] 20000 (0.1%)
G" uncured (Pa)	-	2000 (0%) 10000 (0.05%) [60] 18000 (0.1%)
Dynamic viscosity @ 1 Hz (Pa s)	410 [57]	490 (0%) 860 (0.05%) [60] 1200 (0.1%)
Dynamic viscosity @ 10 Hz (Pa s)	120 [57]	≈400 (all) [60]

layer curing of materials in 3D printing processes. This will reduce the sagging of the printed models. The rheological properties before deposition are very stable as the material only cures under UV exposure. The viscosity was shown unaffected after 2 h [60]. The fast cure potential is also ideal for pairing this material with a conductive silicone composite. The problem of filler dispersion when doing this should be solved. Additional benefits of selecting an addition cure over a condensation cure system include improved mechanical properties, reduced shrinkage and absence of byproducts. Silopren UV LSR 2030 is also said to be skin and food safe which extends applications for fabricated soft actuators. This means it does not suffer from the risk of cytotoxicity found in some photoinitiators [51] used in silicones. Due to its excellent suitability, Silopren UV LSR 2030 was chosen to be the structural material for the 3D printing process.

Table 2.2: A comparison of 3D printable silicones based on the desired characteristics

Material	S1	S2	S3	S4	S5	S6
AMSil 20101	++	++	+	++	+	++
Silopren UV LSR 203	++	++	++	++	++	++

2.3.3 Conductive material

No conductive silicone composites are commercially available. Some ESD silicones are available but these feature resistivities that are too high for sensing applications. A conductive composite will have to be developed for this 3D printing process. Based on the literature study on conductive fillers and the desired characteristics discussed in section 2.3.1, the choice was made to use CB-based fillers. Good resistivity can be achieved at low filler contents when specialised CB fillers are chosen. To make silicone / CB composites compatible with 3D printing rheological modifiers are possibly unnecessary. Obtaining a dispersion with CB should be relatively easy which reduces processing complexity. An added benefit of CB fillers is that they are inexpensive which makes the material to be developed more accessible. CNT fillers were considered (e.g. Tuball 601, an additive specifically designed for silicone compounds) due to their improved performance at low filler content but were deemed unfit due to their carcinogenic potential. AgNP fillers are interesting alternatives, but their minimal benefits for general

sensing applications at the expensive of much higher cost make these materials less interesting for this application.

The size and texture of CB fillers strongly influence the composite's rheological, mechanical, electrical and electromechanical behaviour. CB fillers are composed of agglomerates, which are composed of aggregates, which are composed of individual CB particles (see figure 2.6). The most important factor affecting the electrical of CB is its structure (see figure 2.7). Other factors include particle size and porosity/ void fraction. The agglomerates in high structured CB have long and branched chains [80]. This reduces the required filler content necessary to achieve sufficient conductivity. It also provides higher viscosity, increased modulus, increased hardness and easier dispersion [81]. Smaller CB particles have a larger surface area which increases conductivity [80]. However, a smaller particle size requires increased mixing time and energy [81]. Conductive CB fillers usually show high porosity [81]. The performance of a CB filler is not only dependent on its texture but also on the level of dispersion that can be achieved. The ultimate dispersion is a function of mixing equipment and procedures [81]. CB fillers hinder the curing of silicones. The resulting extended pot life is beneficial for 3D printing. However, too high filler content may cause brittle and uncured materials [73]. The reason for hindered solidification of the silicone was determined to be an insufficient hydrosilylation reaction due to hydroxyl groups found in the CB reacting with silicone-hydrogen groups in the silicone under the influence of its platinum catalyst [82]. Curing speed and the degree of crosslinking were shown to improve by adding hydrogen silicone oil.

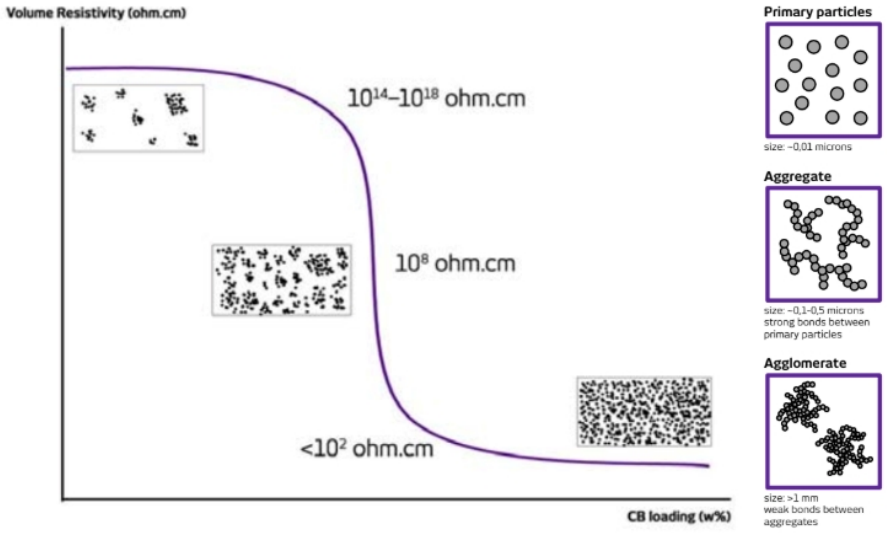

Figure 2.6: CB percolation curve and composition of the filler [80]

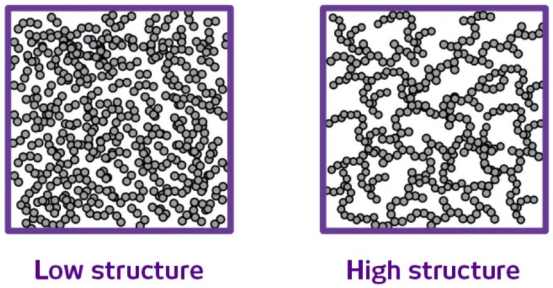

Figure 2.7: Difference between high and low structure in CB fillers [80]

An overview of studies with relevant information on the used silicone matrices, CB fillers and properties of the composite is shown in table 2.3. Ecoflex 00-30 and Sylgard 184 are commonly used silicone matrices. Vulcan XC72(R) and Ketjenblack EC-600JD are commonly used CB fillers. Most contributions are made by K. Aw et al. using Ecoflex 00-30 / Vulcan XC72R [67, 73, 70, 43, 83, 83, 84, 85].

Analysis of the literature showed that current research is lacking in mechanical, electrical and electromechanical characterisation of the materials. Mechanical properties are often regarded as unimportant. Analysis of electrical properties is limited. Either by only mentioning a sensor's resistance without giving dimensions to determine material resistivity, or by mistakenly taking measurements with a multimeter instead of using the 4-wire method during low resistive measurements.

Electromechanical properties of devices such as conductive elastomer strain gauges are strain-rate dependent. Current literature does not consider this and does not mention strain-rate values. This makes a comparison of the found gauge factors impossible. In addition to imperfect characterisation practices, processing methods are generally insufficiently documented making them irreproducible.

Interesting to note is that no literature on condensation cure silicone with CB fillers could be found nor research indicating that these materials are incompatible. Higher possible weight fractions in Ecoflex 00-30 / Vulcan XC72R composites may have been enabled by the improved curing ability side effect of the silicone oil [82] additive whose intended use was to lower the viscosity.

The variety in silicone matrix and CB filler together with the scarcity of reliable data make it impossible to make noteworthy connections. Only three composites were found to enable printing, of which only one composite was shown to have the ability to print three-dimensional structures. Research on 3D printable silicone / CB composites is severely lacking. Development of a silicone / CB composite for soft sensors with intricate characterisation of its various properties made using a reliable reproducible method of processing is highly needed to progress the 3D printable sensor materials research field.

Table 2.3: Silicone / CB composites in literature

Matrix	CB	Content (wt%)	Resistivity (Ω cm)	Gauge factor (resistive)	Rheology modifiers	printable	Source
Ecoflex 00-30	Vulcan XC72R	16.67	-	-	silicone oil	2D	[67]
		8.33	200	-	-	no	[73]
		16.67	-	2.85-3.32	silicone oil	2D	[70]
		12.5-20	-	1.63-1.75	silicone oil	2D	[43]
		5-10	≈10-140*	-	silicone oil	2D	[83]
		5	-	-	-	no	[84]
		10	-	-	-	no	[85]
	Vulcan P	13.04	-	-	-	no	[86]
	Ketjenblack EC-300J	9.09	-	1.62-3.37	-	no	[66]
Sylgard 184	Acytelene	25	22.8	-	-	no	[64]
	Ketjenblack EC-300J	4	-	-	fumed silica	2D	[87]
	Ketjenblack EC-600JD	4,5,6	-	5.696	-	3D	[68]
	SUPER C65	8,10	≈7000-8000	-	-	no	[88]
	Vulcan XC72R	20	-	-	-	no	[89]
	Vulcan XC72	14.3	-	-	-	no	[90]
Neukasil RTV-23	Ketjenblack EC-600JD	12,22	8.33,1.85	-	-	no	[91]
Elastosil LR6200	Ketjenblack EC-600JD	1.0-9.0	-	-	silicone oil	no	[77]
Sylgard 186	Black Pearl 2000	9.1	-	-	-	no	[92]

Development of a composite requires selection of a suitable silicone matrix and CB filler. Relevant properties of Ecoflex 00-30 and Sylgard 184 are shown in Table 2.4. These are both addition cure silicones to maintain compatibility with the same cure system chosen structural material. The structural material cannot be used with CB fillers as the CB blocks the UV light needed for curing. The viscosity of the structural material is also too high. The suitability of the matrices is assessed based on relevant desired material characteristics discussed in section 2.3.1

in Table 2.5. Ecoflex 00-30 shows favourable mechanical properties due to its lower hardness and higher ultimate elongation. The viscosity of this material is also slightly lower which allows higher filler contents. No information could be found on the mechanical hysteresis of these materials. Based on the current knowledge, Ecoflex 00-30 was chosen to be the silicone matrix for the conductive silicone composite.

Table 2.4: Properties of two commonly used silicone matrices for silicone / CB composites

Material	Shore hardness	Ultimate elongation (% strain)	Tensile strength (MPa)	Mixed viscosity (Pa s)	Cure time (h)
Ecoflex 00-30	30 Shore 00	900	1.4	3	4
Sylgard 184	50 Shore A	140	7.1	4	48

Table 2.5: A comparison of 3D printable silicones based on the desired characteristics

Material	S1	C1	C2
Ecoflex 00-30	++	++	unknown
Sylgard 184	+	+	unknown

Two potential CB fillers are analyzed: Vulcan XC72 and Ketjenblack EC-600JD. Vulcan XC72 is considered the industry standard whereas Ketjenblack EC-600JD is considered electrical grade [93]. Table 2.6 shows that the particle sizes are identical. The specific surface area of Ketjenblack EC-600JD is higher likely because of the larger porosity [93]. The increased surface area results in a lower percolation threshold [77]. A comparison of the percolation curves of the two considered conductive fillers and N330, a common tire reinforcement CB filler, constructed from manufacturer data is shown in Figure 2.8. It should be noted that percolation graphs are material and processing method dependent.

Table 2.6: Properties of two conductive CB fillers [93]

Filler	Specific surface area (m^2/g)	Particle size (nm)
Cabot Vulcan XC72	254	30
Nouryon Ketjenblack	1250	30

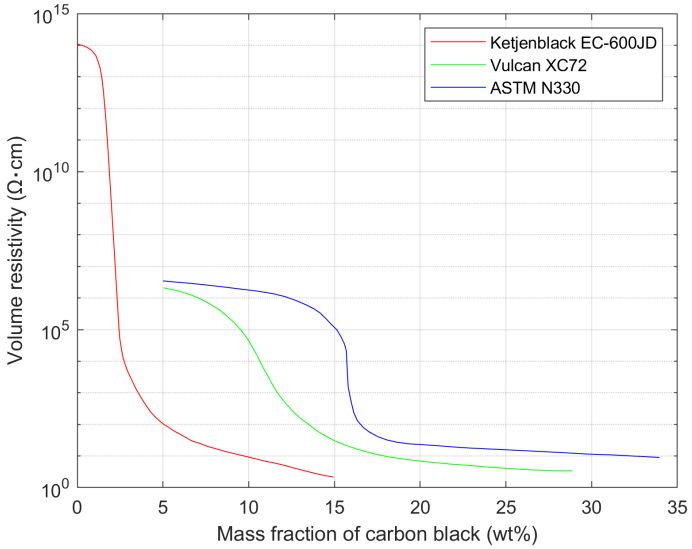

Figure 2.8: CB percolation curves of three CB fillers

The suitability of the CB fillers is assessed in Table 2.7 based on relevant desired material characteristics discussed in section 2.3.1. The lower required filler content for Ketjenblack EC-600JD reduces its effect on mechanical properties and allows lower achievable resistivities. The low structure Ketjenblack EC-600JD has also shown better behaviour for strain sensing applications than elastomers with high structure CB fillers [77]. However, the dispersion of EC-600JD is known to be difficult. Achieving a good enough dispersion for 3D printing applications is uncertain. It was decided to test both CB fillers in experiments on the processing of the material. The better performing CB filler will be used in the conductive silicone composite for the 3D printing process.

Table 2.7: A comparison of CB fillers based on the desired characteristics

Filler	C3	C4	C5	C6
Cabot Vulcan XC72	+	+	++	unknown
Nouryon Ketjenblack	++	++	+	unknown

2.4 Conclusion

This chapter aimed to answer the following research sub-question: "*Which structural and conductive materials comply with the demanding criteria of soft robotics while being compatible with the used DIW 3D printer?*". Silicone type materials were chosen to be the structural material as they exhibit proven favourable characteristics associated with soft robotic applications while being commercially available and requiring minimal processing complexity. Conductive silicone composite type materials were chosen as the conductive material as they are unique in their ability to facilitate complex self-supporting sensing structures both in embedded form and at the surface. Suitable materials of these types were found through a thorough literature review. Silopren UV LSR 2030 was determined to be the most suitable structural material due to its excellent properties and unique ability to quickly cure on demand. Silicone / CB based composites were determined to be best suited for the intended 3D printing process. Ecoflex 00-30 was selected as the silicone matrix due to its excellent mechanical properties and low viscosity enabling the use of higher filler contents without additives. Two fillers, Vulcan XC72 and Ketjenblack EC-600JD, were compared to the desired characteristics. The former shows better performance but the attainability of a good dispersion is uncertain. Both materials will be tested. An analysis on similar silicone / CB approaches showed that characterisation of the materials is lacking and processing of the materials is improperly addressed. Only one study was identified where a silicone / CB composite was used to 3D print three-dimensional structures. Development of a silicone / CB composite for soft sensors with intricate characterisation of its various properties made using a reliable reproducible method of processing is highly needed to progress the 3D printable sensor materials research field.

3 Material processing

3.1 Introduction

Current literature on 3D printing of conductive silicone/CB composites insufficiently addresses methods of processing these materials. One of the improvements of the 3D printing process in this research over others is the inclusion of processing methods. Processing includes mixing and curing of the materials. Mixing is especially important for silicone/CB composites as equipment and procedures strongly influence the outcomes [81]. Obtaining a good dispersion is difficult. The effect of mixing methods and parameters on the properties of the conductive material should thus be studied. This includes electrical and printability properties. The desired outcome of this research is a method that allows dispersion of sufficient quality for the 3D printing process. This method of processing should be reproducible and have minimal complexity.

3.2 Related work

The literature used in Table 2.3 was analysed again, but this time focussing on relevant information of mixing. The results are shown in Table 3.1. Utilized mixer types are the stirrer mixer, planetary centrifugal mixer and three-roll mill. Various additives were used for mixing. Stirrer mixers are suitable for low-viscosity mixtures. Homogeneous dispersion of these mixtures usually takes several hours. Planetary centrifugal mixers are much faster, typically obtaining homogeneous mixtures within ten minutes. They allow the use of both low-viscosity and high-viscosity mixtures. Three roll mills work with high-viscosity mixtures only.

Several additives were used. Solvents used to improve the dispersion of the CB filler in the silicone matrix include ethanol [68], isopropyl alcohol [92], heptane [86], hexane [64, 88], pentanol [87] and toluene [91]. A solvent was used in combination with a stirrer mixer in four out of five cases [86, 64, 68, 88]. The study with Ecoflex 00-30 matrix [86] did not volatilize its solvent before moulding/printing likely because of the faster curing speed compared to Sylgard 184 (4 hours compared to 48 hours). A solvent was used in combination with a planetary centrifugal mixer in two out of five cases [87, 92] (studies by K. Aw [67, 73, 70, 43, 83, 84, 85, 85] are counted as one). The solvents were not volatilized before moulding/printing in both cases. A solvent was likely not necessary with the Vulcan XC72R filler in both Ecoflex 00-30 and Sylgard 184 because of its powder form instead of pelleted/beaded form of the other fillers. Mechanical aid in the form of grinding was used to break down the filler in three cases, of which one used external pre-grinding of the filler [68] and the other two used steel balls in the mixing process [86, 92]. All three fillers are in pelleted/beaded form, which raises the expectation that the dispersion of these types of fillers is more difficult. It should be noted that the quality of dispersion may vary greatly between the shown results. These findings show that various techniques can be used to successfully disperse the filler.

3.3 Selection of a suitable mixer

A suitable mixer had to be chosen to allow synthesis of the conductive silicone composite. Two options were considered; an overhead stirrer mixer and a planetary centrifugal mixer.

The IKA Eurostar 200 is IKA's highest-power overhead mixer designed for highly viscous applications. This mixer has a max viscosity of 100 Pa s. Several stirring elements are available which are optimised for different applications. The 40 mm IKA 1303 dissolver stirrer is recommended for the dispersion of fillers. The mixing volume range of this setup was calculated using the manufacturer's guidelines. The container size and positioning of the stirrer must be carefully

Table 3.1: Silicone/CB composite mixing in literature

Matrix	CB	Content (wt%)	Resistivity (Ω cm)	Mixer	Mix speed (rpm)	Mix duration (h)	Mix additive	Source
Ecoflex 00-30	Vulcan XC72R	16.67	-	planetary centrifugal	-	-	-	[67]
		8.33	200	planetary centrifugal	-	-	-	[73]
		16.67	-	-	-	-	-	[70]
		12.5-20	-	planetary centrifugal	-	-	-	[43]
		5-10	≈10-140	planetary centrifugal	-	-	-	[83]
		5	-	-	-	-	-	[84]
		10	-	-	-	-	-	[85]
	Vulcan P	13.04	-	stirrer	-	0.5+5+0.25 h	heptane, steel balls	[86]
	Ketjenblack EC-300J	9.09	-	planetary centrifugal	2000	0.17	-	[66]
Sylgard 184	Acytelene	25	22.88	stirrer	-	1	acetone/hexane	[64]
	Ketjenblack EC-300J	4	-	planetary centrifugal	2000	0.08+0.08	pentanol	[87]
	Ketjenblack EC-600JD (ground)	4,5,6	-	stirrer	1500	0.5+0.5+?	ethanol	[68]
	SUPER C65	8,10	≈7000-8000	stirrer	-	1+1	hexane	[88]
	Vulcan XC72R	20	-	stirrer	-	0.08+0.05	-	[89]
	Vulcan XC72	14.3	-	planetary centrifugal	-	-	-	[90]
Neukasil RTV-23	Ketjenblack EC-600JD	12,22	8.33,1.85	three-roll mill and stirrer	-	0.17	toluene	[91]
Elastosil LR6200	Ketjenblack EC-600JD	1.0-9.0	$<1\times10^{5}$	three-roll mill	-	0.17	-	[77]
Sylgard 186	Black Pearl 2000	9.1	-	planetary centrifugal	2000	0.17	IPA, steel balls, isooctane	[92]

chosen as they strongly influence the effectiveness. The calculations yield a minimum mixing volume of 201 mL and maximum volume of 1266 mL.

The second considered option is to use a Hausshild Speedmixer DAC 150 planetary centrifugal mixer. This mixer can process both low-viscosity and high-viscosity mixtures without being in contact with the material itself. The material is loaded into a cup. This cup moves around an arm while being rotated around in the opposite direction around its axis at a 45 degree angle. This combination causes high shearing forces and material flow in the cup. This method is very effective for high-viscosity formulations. These mixers have even been demonstrated homogeneously mixing of clays. An added benefit of these mixers is that their operational principle causes degassing of the mixture as well. This is a desirable property since alternatively adding a vacuum chamber treatment would reduce the working time of the conductive material. The DAC 150 mixer has a mixing range of 5 g to 100 g which equates to 4.7 mL to 94 mL given Ecoflex 00-30's specific volume of 0.94 $cm^3\,g^{-1}$.

An overview of the mixers is shown in table 3.2. The viscosity of the structural material, Silopren UV LSR 2030, was shown to be higher than the 100 Pa s limitation of the stirrer mixer [60]. The conductive composite is expected to have similarly high viscosities under high filler content. The syringes of the Brinter's tool heads have a volume of 10 mL. The minimum batch size with the stirrer mixer would be far too big. For these reasons, the choice was made to purchase a DAC 150.

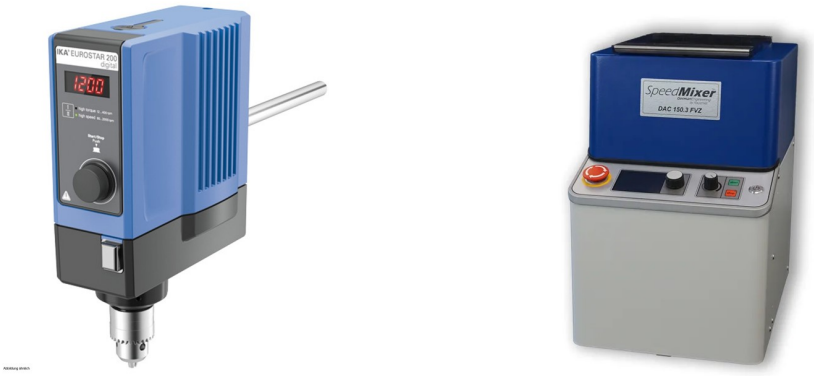

Figure 3.1: IKA Eurostar 200 stirrer mixer and Hausshild Speedmixer DAC 150 planetary centrifugal mixer

3.4 Attempts at dispersing the CB fillers

Obtaining a good dispersion of CB fillers is difficult. Various approaches inspired by literature will be tested to find a suitable processing method. Both CB fillers were provided by their man-

Table 3.2: Properties of two commonly used silicone matrices for silicone/CB composites

Product	Mixer type	Maximum viscosity (Pa s)	Volume range (mL)
IKA Eurostar 200 + 1303	stirrer	100	201-1266
Hausshild Speedmixer DAC 150	planetary centrifugal	unlimited	4.7-94

ufacturer. Vulcan XC72 is a filler that is compacted into beads of approximately 1 mm in size. Ketjenblack is a filler that is compacted into pellets of approximately 3 mm in size. These beads/pellets are to be broken down into agglomerates. High shear forces are necessary to obtain a good dispersion of these agglomerates in the silicone matrix.

3.4.1 Methods

Methods used in relevant literature included mixing without solvents, mixing with solvents, mixing with solvents and grinding media, and grinding the filler before mixing. Three approaches were tested with the chosen silicone matrix and CB filler. These approaches are:

1. Mixing without solvents: Three sequences of adding the CB filler, silicone part A and silicone part B were tested.
   (a) Sequence 1: Add silicone part B to a cup. Add the CB filler. Mix at 2000 rpm for 2 min. Add silicone part A to the mixture. Mix at 2000 rpm for 2 min.
   (b) Sequence 2: Add the CB filler to a cup. Add the silicone part B and wait 30 min. This may improve the impregnation of the silicone before mixing. The subsequent steps were identical to those of sequence 1.
   (c) Sequence 3: Add CB, silicone part A and silicone part B together. Then mix for 2x2 min at 2000 rpm. The mixture is allowed to cool down between mixing.
2. Mixing with solvent (isopropyl alcohol (IPA)): IPA was added to the mixture with a weight ratio of 1:1.5:1 (IPA:Ecoflex part B:XC72). Various mixing speeds and durations were tested.
3. Mixing solvent (IPA) and grinding media: ten steel balls (6 mm) were used to to aid in breaking down the pellets/beads. They were added with Ecoflex part B and mixed at 2000 rpm for 5 min. Thereafter, Ecoflex part A was added and mixed at 2000 rpm for 2 min. The balls were removed using a magnet after which the composite was mixed again for 2 min at 2500 rpm.

Ecoflex is a 1:1 ratio two-component addition cure silicone that cures quickly. It was found that the material could cure within 5 min when mixing due to heat produced from friction. CB fillers slow down the curing process sufficiently to make the composite compatible with the Speedmixer and subsequent 3D printing. The CB filler was added to part B because it has a lower viscosity than part A. Isopropyl alcohol was chosen as a solvent because it was available in the lab and shown in literature [92]. The lab has no experience with more purpose-fit solvents such as heptane, hexane and toluene. The use of these solvents was opposed and therefore not tested. The weight range for the Speedmixer is dependent on the chosen cup and holder. The optimal fill range for the PP50 90 mL cups chosen for mixing is 25 g to 65 g.

3.4.2 Results and discussion

Mixing without solvents did not yield satisfactory results. Multiple combinations of mixing speed and duration were tested. A filler content with a mass fraction of 10.5 % was used for Vulcan XC72. The same filler content was tested with Ketjenblack EC-600JD but this caused a

much more viscous paste that was almost clay-like. The filler content was adjusted to a mass fraction of 6.25 % to obtain a compatible viscosity to that of Vulcan XC72 mixture. Vulcan XC72 filler beads remained visible in the mixture as shown in Figure 3.2. No difference was found between the sequences, all were unable to disperse the CB filler successfully. Higher mixing speeds and longer duration did not improve the dispersion. Higher mixing speeds cause a rapid increase of temperature due to the increased friction. At low filler content, this could easily lead to premature curing. This was observed at a mixing speed of 3500 rpm. It is important to cool the mixture between mixing steps to minimize this. Mixing durations beyond a total of 4 min did not alter the texture of the mixture. The breakdown of Ketjenblack EC-600JD filler pellets during mixing was better. The texture of the mixture visually changed over time. Mixing beyond 4 min also did not improve the dispersion. It is clear that mixing with only the matrix filler did not obtain the desired dispersion. The clumped agglomerates in the mixture will clog the nozzles when printed and the bad dispersion will cause a higher resistivity for the given mass fraction.

Figure 3.2: Results after mixing for 2x2 min at 2000 rpm

IPA was added to the mixture to improve the dispersion. Mixing was tested at various speeds and durations but the filler failed to disperse. The beads were unable to (fully) break down into agglomerates. It was observed that this breakdown was slightly better in higher viscosity mixtures likely caused by the interaction of the beads.

An attempt was made at adding mm diameter steel balls to the process. The hope was that this would aid in breaking down the Vulcan XC72 beads. This idea was inspired by other research [92]. The dispersion did not improve over the case when only IPA was used. The paper used iso-octane as well which likely had a crucial role in obtaining a good dispersion. Higher energy methods are necessary for the breakdown of pellets/beads into agglomerates.

3.5 Grinding of the CB filler to improve the dispersion

One study that was discussed ground the CB filler before use [68]. This may potentially be the solution to improve the breakdown of pellets/beads into agglomerates.

3.5.1 Methods

The CB filler is ground prior to mixing. The Speedmixer is operated as a ball mill. This is a recognized application of the Speedmixer and accessories that do this have been developed [94]. Polypropylene (PP) or aluminium cups are typically used. Standard Speedmixer PP cups were used in this experiment.

Yttria-stabilized zirconia pearls (1.5 mm) were recommended by Speedmixer representatives based on our application. The cup was filled with 10 g of XC72 filler and 50 g of grinding media. Figure 3.3 shows that the volume of grinding media is much low than that of CB filler while its mass is much higher, indicating a much higher density. The total weight is within the optimal fill range (55 g to 105 g) for the used PP100 185 mL cup. The bigger cup solved problems with compacting of the powder during grinding experienced with a PP50 cup. The contents were ground for 1 min at 2000 rpm. Big particles and the zirconia pearls were removed from the resulting powder by sifting using a tea sift (see Figure 3.4). This should be conducted in a fume hood for safety purposes.

A PP50 mixing cup was loaded with 3.5 g filtered XC72 powder and 15 g Ecoflex part B. This was mixed for 2 min at 3000 rpm three times with cooling using a cup filled with cold water in-between for 1 min. The cooling should extend the pot life. The same amount of Ecoflex part A was added and the combination was mixed for 2 min at 2000 rpm twice with cooling in-between for 1 min. Figure 3.5 shows that the volume of the filler is approximately four times greater than that of the silicone while having a mass that is four times lower, indicating a much lower density. After obtaining the mixture, extrusion of the material using the Pneuma Tool was attempted.

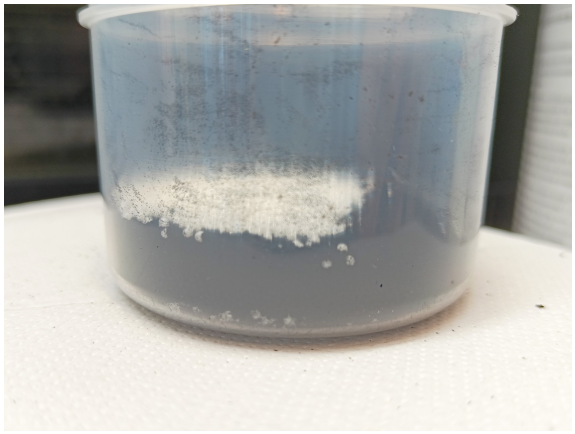

Figure 3.3: 10 g of XC72 filler and 50 g of grinding media added to a PP100 cup

Figure 3.4: Seperation of powdered filler using a tea sift

3.5.2 Results and discussion

Grinding generated heat due to friction. Grinding speed and duration should be carefully chosen. Too much heat generation could damage the cup and release CB powder. Grinding for 1 min at 2000 rpm raised the temperature of the cup sufficiently for it to be uncomfortable to

Figure 3.5: 15 g of Ecoflex part B (clear) added to 3.5 g of filtered powdered Vulcan XC72 (black)

hold. The dispersion shown in Figure 3.6 shows a major improvement over earlier attempts. Some dots are visible but these are likely clumped agglomerates. The dispersion is thus not yet optimal. Additional grinding and mixing may improve the dispersion.

Figure 3.6: Dispersion of Vulcan XC72 and Ecoflex 00-30 (mass fraction of 10.5 %)

Earlier dispersions were not able to be extruded due to immediate clogging of the syringe tip. A syringe was loaded with the dispersion. A 0.41 mm tip was selected as this size is closest to nozzles commonly used in FFF printing. Extrusion of the material was possible at a pressure of 1450 mbar. Extruded material is shown in figure 3.7. The tip clogged after approximately half of the syringe, 5 mL, was extruded. Additional experimentation with mixing and grinding may improve the dispersion to a point that clogging does not occur any more. The effect of grinding and mixing parameters on the printability of the dispersion should be studied.

3.6 The effect of grinding and mixing parameters on material properties

A structured approach is necessary to determine a method of grinding and mixing that produces homogeneous dispersions suitable for use in the 3D printing process. Insufficient grinding and mixing leads to poor resistivity and clogging of the printing system during extrusion. The parameters that influence the dispersion are grinding speed, grinding duration, mixing speed, mixing duration, and cooling measures. The goal of this experiment is to study the effect of these parameters on the resistivity and printability of the material. Experiments are performed using both filler types.

Figure 3.7: Extrusion of the dispersion with a 0.41 mm tip

3.6.1 Methods

The performance of the fillers will be tested by choosing formulations that are expected to have the same resistivity. Low-content formulations should not be a problem with either of the fillers. Therefore, this experiment will test a high filler content, which implies a low resistivity. Figure 3.8 shows the percolation graphs of the fillers. The behaviour of the logarithmic percolation graph could not be described by curve fitting tools. Instead, curve fitting was attempted in the area of interest shown by the linear zoomed-in percolation graph. Polynomial curve fitting was unable to describe this behaviour as well. The solution was to implement a two-term exponential model for the fit. This model can describe the behaviour with high accuracy. The fits were used to predict the required filler content to obtain a resistivity of 100 Ω cm. This resulted in a filler content with a mass fraction of 13.48 % for Vulcan XC72 and 5.06 % for Ketjenblack EC-600JD.

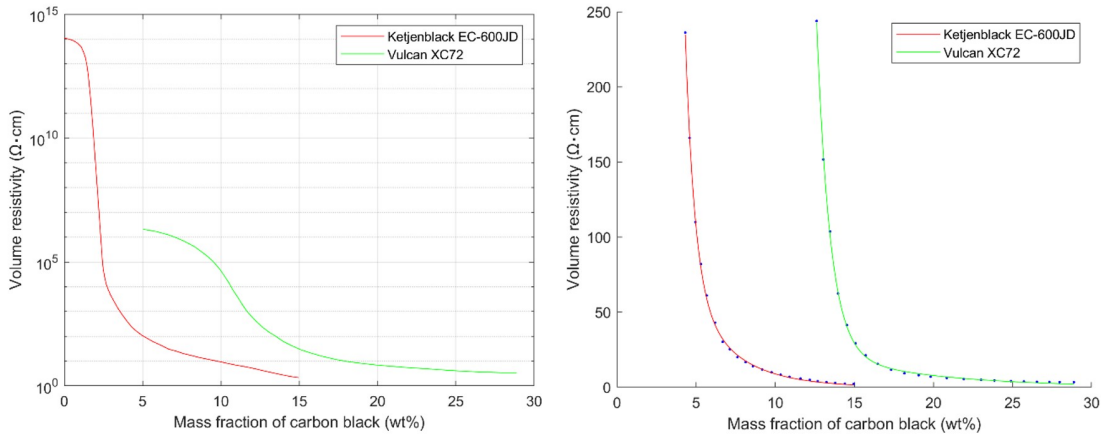

Figure 3.8: Percolation graphs of the fillers **(left)** logarithmic scale **(right)** linear scale zoomed in to 0 Ω cm to 250 Ω cm

A PP100 cup was used, to which 7 g of CB and 50 g of zirconia pearls were added. The Ketjenblack EC-600JD filler takes on a large volume when ground. Adding more than 7 g Ketjenblack EC-600JD is not recommended as compacting of the powder was observed which affects grinding performance. The grinding speed was set to 1500 rpm. This speed is good as it does not create too much heat due to friction yet allows for sufficient grinding. The fillers were ground for 1 min five times with cooling for 1 min in between. This was necessary as temperatures rose to 60 °C within a minute. The powder was cooled down to 45 °C after every minute. The long grinding duration should break down the pallets/beads better than the 1 min grinding dura-

tion tried earlier. After grinding, the ground filler was separated from the zirconia pearls and the remaining pellets/beads using a tea sift. The fillers before and after grinding are shown in Figure 3.9 and figure 3.10.

Figure 3.9: Vulcan XC72 before and after grinding

Figure 3.10: Ketjenblack EC-600JD before and after grinding

Three variations were tested for each filler. First, mixing with a speed of 2000 rpm was attempted without grinding. Second, mixing with a speed of 2000 rpm was attempted with grinding. Third, mixing with a speed of 3000 rpm was attempted with grinding. The resistance within the mixture is measured to determine the ideal mixing duration. The following steps were taken for each of the six samples.

1. Add the CB filler and both Ecoflex parts to the cup.
2. Mix at 2000 or 3000 rpm for 30 s. Take the cup out of the Speedmixer and measure its temperature. Wait for the mixture to cool down to 45 °C to take a resistance measurement within the cup using the tool shown in Figure .
3. Repeat the step above nine more times for a total mixing time of 300 s.
4. Transfer material from the cup to a syringe. Measure the material flow at a pressure of 5000 mbar. This is the maximum safe pressure of the Pneuamtool.
5. Transfer material from the cup to 3 moulds with electrodes. Measure resistance 30 min thereafter.
6. Cure moulds in the oven at 80 °C for 20 h. Measure the resistance afterwards.

The CB filler and both Ecoflex parts were added to the cup together rather than in two steps because the mixture with Ketjenblack experienced problems. The highly viscous mixture caused the formation of spheres which would not mix after the addition of Ecoflex's second part (see Figure 3.11). Suspicions that the mixture may cure prematurely by applying this method did not become reality. This is likely due to the filler dispersion quickly, hindering the curing process sufficiently. The mixing duration was split up into parts of 30 s to minimise the rise in temperature.

Figure 3.11: Ketjenblack EC-600JD before and after grinding

A tool was developed to measure the resistance within the cup (see Figure 3.12). This tool was FFF 3D printed with polyethylene terephthalate (PETG). In combination with a measurement system, this tool enables a 4-wire resistance measurement of the uncured material in the cup. The application of a 4-wire measurement is crucial to eliminate the contact resistance of the electrodes with the material. A multimeter (model DAQ6510, Keithley) was used for the 4-wire resistance measurements.

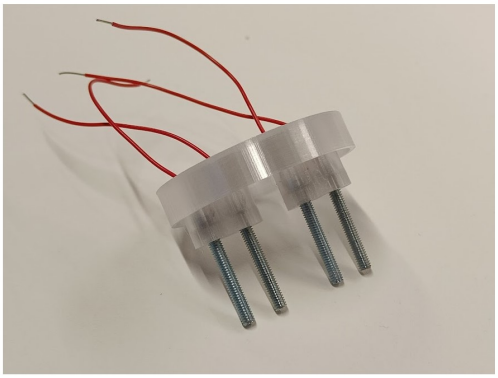

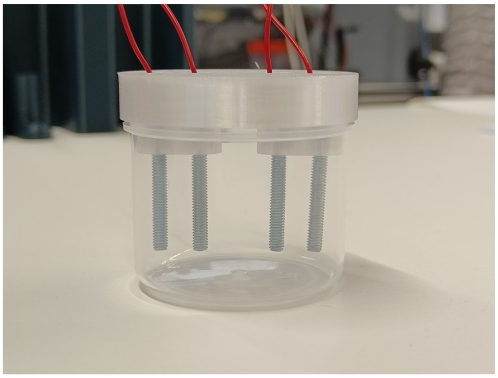

Figure 3.12: Developed tool to enable 4-wire resistance measurements on the uncured material

Brinter's tools use 10 mL syringes. Loading these with highly viscous materials is difficult by hand. G. Wolterink developed a special tool to make this process easier (see Figure 3.13). This tool can transfer materials directly from the Speedmixer cups into the syringe without air pockets in the syringe. A piston with larger tolerance (Nordson EFD Beige SmoothFlow) was used as the tolerance of standard pistons (Nordson EFD White SmoothFlow) was too small causing the piston to get stuck to the walls. The loaded syringes were connected to the Pneumatool. The material flow was measured using a high precision single point load cell (Model 1004, Vishay Tedea-Huntleigh) and read out using a USB DAQ (DEWE-43A)(see Figure 3.14). This will verify whether the material flow over time is constant.

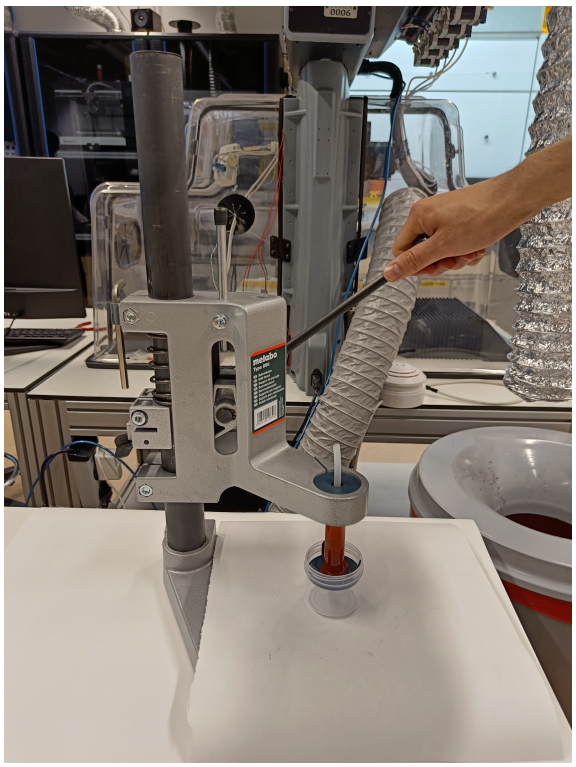

Figure 3.13: Developed tool for loading a syringe with mixed materials

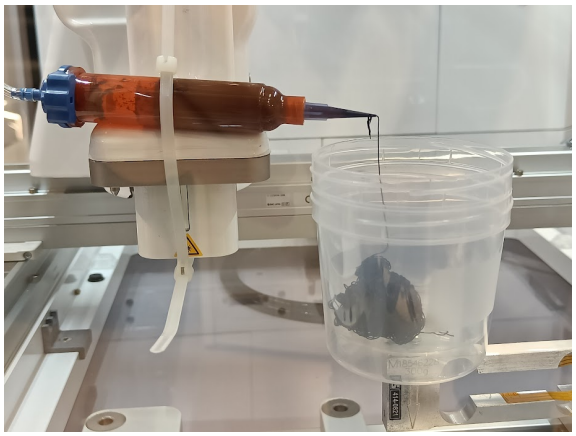

Figure 3.14: Measurement of material flow using a load cell

Measuring the resistivity of the material in a reliable manner requires casting the material in a predetermined shape. A design for a mould was made (see figure 3.15). It features four spots for electrodes to allow a 4-wire resistance measurement. An accurate multimeter (model DAQ6510, Keithley) was used for these measurements. The distance between the two inner electrodes is exactly 20 mm. The cross-section of the slot for the material is 5 mm by 3 mm. The resistivity can be determined using the resistance measurement and these dimensions. The moulds were fabricated from PETG using FFF 3D printing. PETG was chosen because it has better chemical resistance and higher glass transition temperature compared to polylactic acid (PLA). The higher temperature resistance allows the use of higher cure temperatures.

Casting of silicones in 3D printed moulds can give problems. The porous structure can trap silicone and cure inhibition at the interface can occur. These problems can be minimised with the use of a mould release agent. Typical mould release agents contain silicone ingredients. These are not suitable for this application as they would affect the silicone elastomer. Mann

Easy Release 200 is a release agent that is suitable for use with silicones. Figure 3.17 shows that this release agent works effectively with the developed material. The release agent solved the stickiness of the material at the interfaces with the mould.

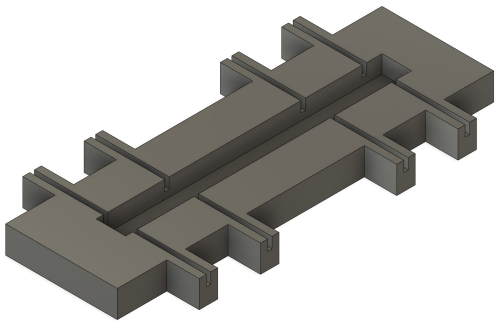

Figure 3.15: Design of the moulds used for determination of the resistivity

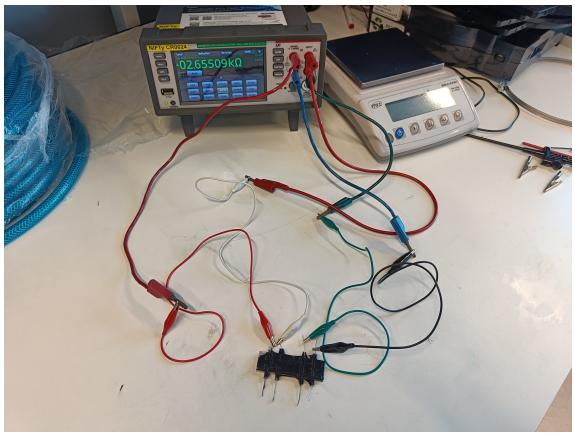

Figure 3.16: Resistance measurement with the Keithley DAQ6510

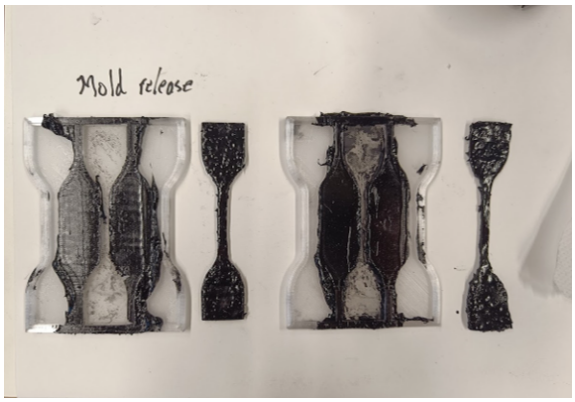

Figure 3.17: A silicone part cast in a mould with and a mould without Mann easy release 200

After casting the material in the mould, both are transferred to an oven. The curing progress of the silicone is hindered by the CB filler [82]. Curing at room temperature can take hours to weeks depending on the filler content. The cure of addition cure silicones can be accelerated with heat. A variety of temperatures and cure times were used to cure silicone/CB composites in literature (see table 3.3). A temperature of 80 °C was selected for this experiment. Higher temperatures caused the PETG mould to deform during the curing process. The cure time was

set to 20 h. Longer cure times were found to be undesired for the 3D printing process. Materials that are unable to cure within this time are considered unsuitable.

Table 3.3: Silicone/CB composite curing in literature

Matrix	CB	Content (wt%)	Temperature (°C)	Duration (h)	Source
Ecoflex 00-30	Vulcan XC72R	16.67	RT	12	[67]
		8.33	50	10	[73]
		16.67	RT	-	[70]
		12.5-20	-	-	[43]
		5-10	-	-	[83]
		5	40	2	[84]
		10	80	12	[85]
	Vulcan P	13.04	RT	24	[86]
	Ketjenblack EC-300J	9.09	80	0.5	[66]
Sylgard 184	Acytelene	25	130+RT	0.42(oven)+48(RT)	[64]
	Ketjenblack EC-300J	4	-	-	[87]
	Ketjenblack EC-600JD	4,5,6	-	-	[68]
	SUPER C65	8,10	RT	24	[88]
	Vulcan XC72R	20	70	-	[89]
	Vulcan XC72	14.3	120	0.17	[90]
Neukasil RTV-23	Ketjenblack EC-600JD	12,22	80	4	[91]
Elastosil LR6200	Ketjenblack EC-600JD	1.0-9.0	100	100	[77]
Sylgard 186	Black Pearl 2000	9.1	80	0.5	[92]

3.6.2 Results and Discussion

The experiments were performed on both Vulcan XC72 and Ketjenblack EC-600JD. Figure 3.18 shows the progression of the resistance with mixing duration for both fillers. The results containing mixtures with unground filler are excluded as they showed much higher resistances. Increasing the mixing speed from 2000 rpm to 3000 rpm resulted in improved dispersion. Figure 3.19 shows the appearance of the mixtures after the test. The grinding and increased mixing speed improved the dispersion. The amount of clumps that can be seen is reduced. The optimal dispersion was achieved within the tested period. The lowest resistance was achieved at a different point for every filler and mixing speed combination. Both materials quickly approach their minimum resistance. However, a visual assessment revealed that a majority of the clumps were still present at short mix durations. A mixing duration that works well for both materials and should cause minimal clumps is 210 s. This is shorter than was shown in literature (see table 3.1). It should be noted that the depth of the probes influences the resistance. Some material is removed from the cup when removing the tool for mixing. This increases the measured resistance slowly over time.

The materials were cast into the moulds and cured. A major finding was that the mixtures with Vulcan XC72 failed to cure within 20 h. The high filler content that was tested is unsuitable for our application. Improved curing behaviour is expected at lower filler content. The mixtures containing Ketjenblack EC-600JD cured successfully. The resistivity was determined before and after the curing process. The results are shown in Table 3.4. These can be compared to the predicted resistivity of 100 Ω cm. Mixtures of both fillers performed poorly when no grinding was applied. Vulcan XC72 surpassed the prediction when a mixing speed of 3000 rpm was used. Ketjenblack EC-600JD performed much better than expected. The resistivity was less than a fifth of the predicted value when a mixing speed of 3000 rpm was used. Figure 3.20 shows the results in relation to the predicted percolation graphs. The measured resistivities were lower after the curing process.

The materials that included grinding of the filler were successfully extruded using the Pneuma Tool with a pressure of 5000 mbar. Unground filler materials failed to extrude. Figure 3.21 shows the extruded amount of material over time. Vulcan XC72-based mixtures showed a

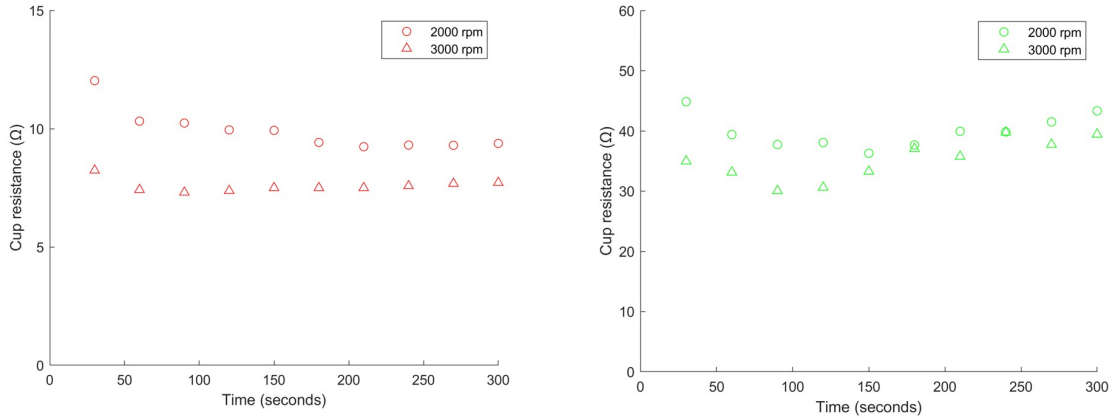

Figure 3.18: Cup resistance measurements as a function of mixing duration **(left)** Ketjenblack EC-600JD **(right)** Vulcan XC72

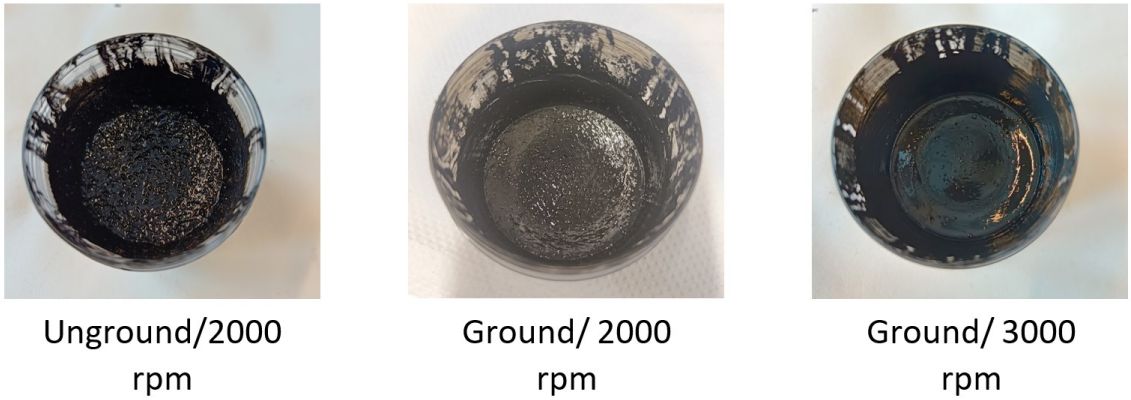

Figure 3.19: Vulcan XC72 based compositions after mixing

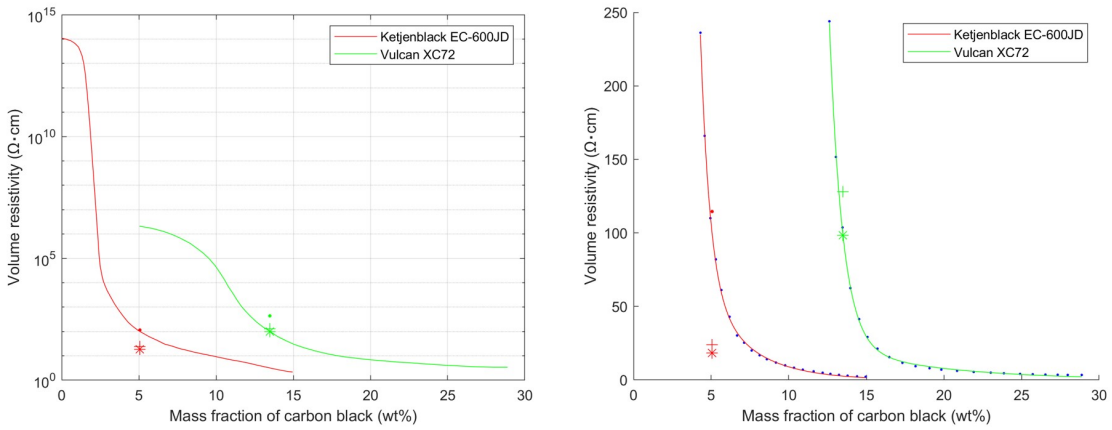

Figure 3.20: Resistviy results after curing. Unground is indicated by ·, Ground/2000 rpm is indicated by +, Ground/3000 rpm is indicated by ∗.

higher material flow indicating a lower viscosity. The viscosity of Ketjenblack EC-600JD is much more sensitive to mass fraction. Ketjenblack EC-600JD mixed at 3000 rpm does not show a consistent extrusion. However, this was caused by clogging of the tip. The used piston got stuck to the inside of the syringe at approximately 800 s which affected the experiment. The flow

Table 3.4: Silicone/CB composite curing in literature

CB filler	Grinding/Mixing	Resistivity before cure average (Ω cm)	Resistivity after cure average (Ω cm)
Ketjenblack EC-600JD	no/ 2000 rpm	156.28	114.55
	yes/ 2000 rpm	24.84	23.81
	yes/ 3000 rpm	20.37	18.31
Vulcan XC72	no/ 2000 rpm	495.27	436.40
	yes/ 2000 rpm	140.93	128.15
	yes/ 3000 rpm	143.16	98.42

stabilised again after this incident. The flow measurements show that the tested grinding and mixing parameters are successful at creating a dispersion that has stable flow properties.

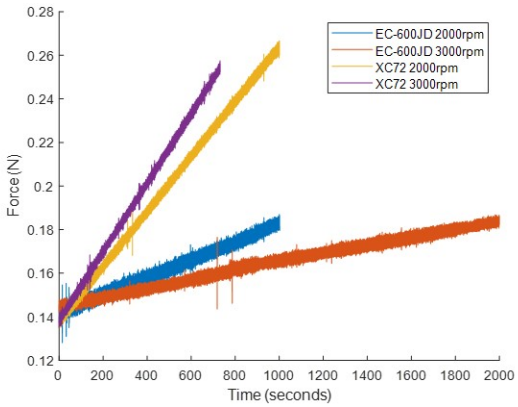

Figure 3.21: Material extrusion over time with a 0.41 mm tip at a pressure of 5000 mbar

3.7 Conclusion

This chapter aimed to answer the following research sub-question: *"How can the selected materials be processed successfully using a method with minimal complexity?"*. Typical high power overhead stirrers are unable to process the high viscosity mixtures used in this research. A Hausshild Speedmixer DAC 150 planetary centrifugal mixer was selected instead. This mixer is able to quickly process both low viscosity and high viscosity mixtures in the batch sizes required for this application. Initial attempts at dispersing the CB fillers failed. The mixing action was insufficient to break down the palleted/beaded form of the fillers into agglomerates. The solution was found by grinding the CB filler into powder using zirconia pearls before mixing. The improved dispersion enabled extrusion for 3D printing. Attempting to synthesize and cure materials with a predicted resistivity of 100 Ω cm showed that mixtures with Vulcan XC72 could not cure. A reduction of filler content will be necessary when using this filler. Mixtures using Ketjenblack EC-600JD exhibited reduced impact on the curing process due to the lower required filler content. Mixtures based on this filler also showed resistivity values that were a fifth of those seen with Vulcan XC72 which approached the predicted value. Increasing the mixing speed from 2000 rpm to 3000 rpm lowered the resistivity and improved the dispersion. All mixtures that involved grinding showed a sufficient dispersion quality for stable extrusion. The recommended procedure to successfully grind the CB filler, disperse the powdered CB filler in Ecoflex 00-30, and load the dispersion into a syringe is described in table 3.5.

Table 3.5: Recommended processing procedure.

Step	Action	Notes
G1	Add 7 g of CB filler and 50 g zirconia pearls to a PP100 cup.	Higher speeds may lead to compacting of the powder during grinding.
G2	Set the Speedmixer to mix at 1500 rpm for 1 min.	Higher speeds reach temperatures possibly damaging the cup.
G3	Wait for the cup to cool down to 45 °C	A cup containing cold water can be used to enhance cooling.
G4	Repeat steps G2 and G3 four more times.	
G5	Separate the powdered filler using a tea sift.	This should be conducted in a fume hood.
G6	Transfer powdered CB filler to a cup for storage	Double bag this cup.
M1	Calculate the required amount of CB filler based on a combination with 30 g silicone.	Lower silicone amount reaches the lower limit of the Speedmixer.
M2	Transfer the desired amount of powdered CB filler to a PP50 cup.	This should be conducted in a fume hood.
M3	Transfer 15 g Ecoflex part A and 15 g Ecoflex part B to the cup.	Use separate tools to avoid contamination.
M4	Set the Speedmixer to mix at 3000 rpm for 30 s.	Higher speeds may induce too much heat.
M5	Wait for the mixture to cool down to 45 °C	A cup containing cold water should be used to enhance cooling.
M6	Repeat steps M4 and M5 six more times.	This should be sufficient for a homogeneous dispersion.
S1	Prepare the syringe loading tool as shown in figure 3.13.	Required materials are a 10 mL syringe, 3D printed plunger and piece of tube.
S2	Install the cup in the syringe loading tool and pull the handle.	Apply force slowly to prevent air bubbles from forming in the syringe.
S3	Remove the syringe from the loading tool and install a piston.	Nordson EFD Beige SmoothFlow should be used for its higher tolerance.
S4	Add a tip of a desired size to complete the syringe.	Nordson EFD Smoothflow tapered dispense tip (Gauge 22/ 0.41 mm) is recommended

4 Material characterisation

4.1 Introduction

The material processing chapter showed that Ketjenblack EC-600JD showed better electrical properties while minimally affecting the curing behaviour. For this reason, it was selected for use in the 3D printing process. As was shown in section 2.3.3, the current literature insufficiently and incorrectly characterises developed silicone / CB materials. This study aims to analyse the electrical, mechanical, electromechanical and printability properties of the developed silicone / CB composite. This includes the effect of filler content on these properties. The findings should give an understanding of the limitations of this material and aid in making informed choices on filler content in future uses.

4.2 Methods

Only Ketjenblack EC-600JD filler is used in this study. To understand the effect of filler content, a variety of formulations were tested. These are 3.5 wt%, 4.0 wt%, 4.5 wt%, 5.0 wt% and 5.5 wt%. These materials were synthesised using the procedure described in Table 3.5. The materials were cured for 24 hours at a temperature of 80 °C.

The electrical property of the material to determine is resistivity. Resistivity measurements were accomplished using the method that was introduced in section 3.6.1. Three moulds were filled for each formulation. The method was extended by adding a moment of measurement after the removal of the samples from the mould. Variation in the measurements should be reduced due to the removal of excess material. After removing the samples from the moulds, they were strained to 50% five times and laid to rest overnight (removal shown in Figure 4.1). The purpose of this is to have a fairer comparison as removal from the mould resulted in more stress applied to some samples than others which could have affected the conductive networks.

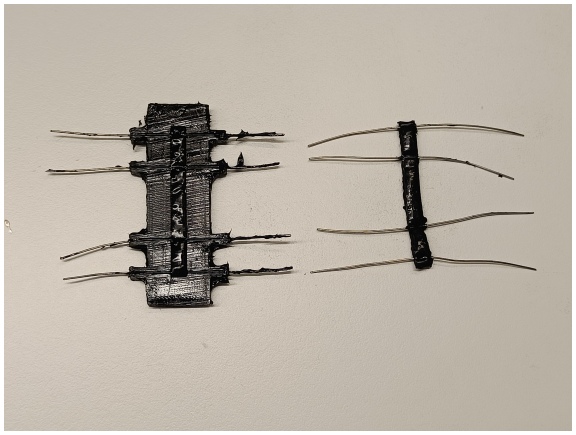

Figure 4.1: Removal of the samples from the mould.

The mechanical behaviour of the material is of interest in order to assess its suitability for soft robotic applications. Relevant properties are Young's modulus and mechanical hysteresis caused by viscoelasticity. The evolution of these properties under the influence of various degrees of filler content is to be studied. Determining these properties requires controlled axial straining of the material. A test setup was built in collaboration with G. Wolterink (see Figure 4.2). This setup uses a linear actuator (SMAC, model LDL40-100-31-3F) with motor controller (SMAC, model VLC-M1), high precision single point load cell (Vishay Tedea-Huntleigh, model 1042 (5 kg)), and 3D printed clamps to secure the sample. The clamps were designed such that the cured samples can be used in this setup. Cavities on the side of the clamp hold the elec-

trodes in place during the experiments. The clamps were designed such that the samples were secured with minimal force (see Figure 4.3). The force experienced by the load cell and the displacement of the actuator were recorded synchronously using a USB DAQ (DEWE-43A). The load cell measurements were filtered using a 90 Hz low pass filter to reduce noise.

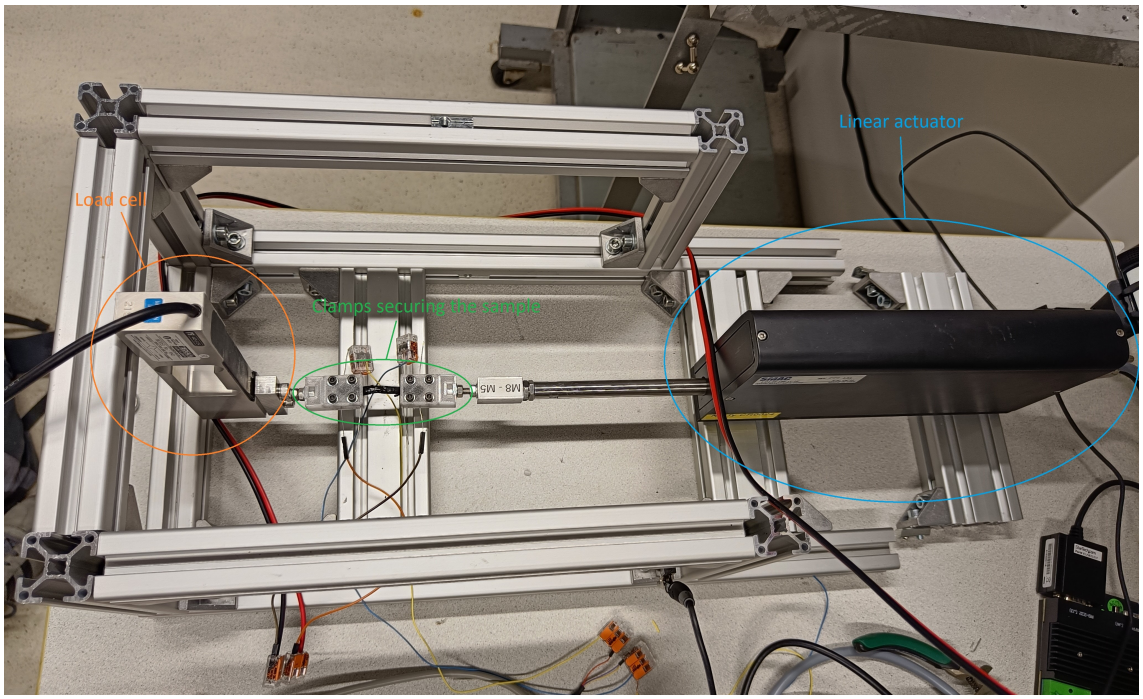

Figure 4.2: Test setup used for mechanical and electromechanical characterisation of the mateterial.

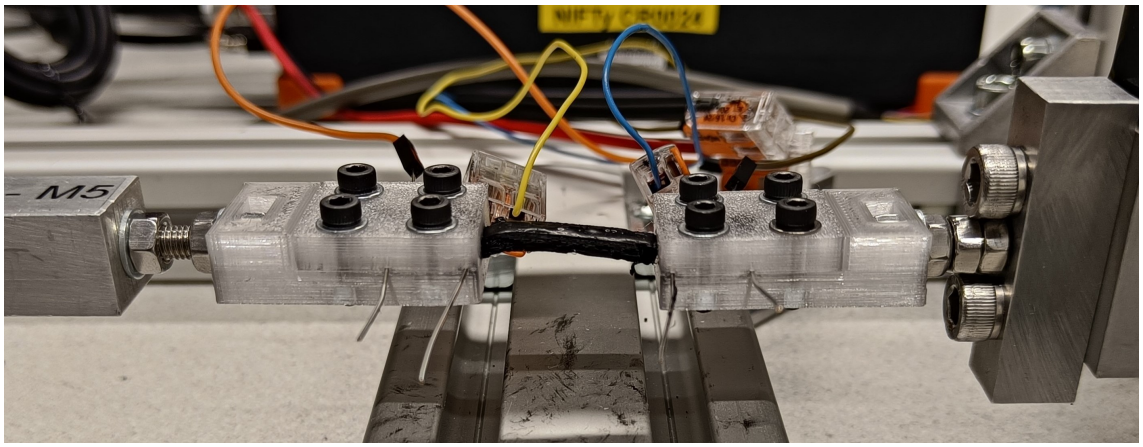

Figure 4.3: Clamps securing the sample.

Electromechanical characterisation is conducted using the same test setup as used for mechanical characterisation. Relevant properties are the gauge factor and electromechanical hysteresis. A 4-wire resistance measurement was applied to the sample to eliminate contact resistance. This was achieved by applying a 100 µA constant current over the outer electrodes using a source measure unit (Model 2450, Keithley). The resulting voltage drop over the inner electrodes was recorded synchronously with the force and displacement using the USB DAQ (DEWE-43A).

A MATLAB (The Mathworks Inc.) script to initialise the linear actuator and program trajectories was developed in collaboration with G. Wolterink. A list of the tested trajectories is shown in Table 4.1. The tests were run for 10 periods. Low frequency (0.05 Hz) and high frequency (0.5 Hz)

triangular waves were applied for the measurement of Young's modulus and the gauge factor. Both properties are strain-rate dependent for conductive viscoelastic materials. A triangular wave is best suited for studying these properties due to its constant strain nature. Sinusoidal waves with the same two frequencies were also tested. These can be used to study viscoelasticity through dynamic mechanical analysis in the future. In the end, a triangle wave with a peak-peak amplitude of 200% was tested to determine whether the materials were capable of these high strains without plastic deformation.

Table 4.1: Tested trajectories

Trajectory identifier	Trajectory type	Frequency (Hz	Peak-peak amplitude (strain %)	Strain rate (%/s)
E1	Triangle wave	0.05	50	5
E2	Sinusoidal wave	0.05	50	-
E3	Triangle wave	0.5	50	50
E4	Sinusoidal wave	0.5	50	-
E5	Triangle wave	0.05	200	20

The printability of the material was tested using the same method that was applied in section 2.3.3. Both a 0.41 mm tip and a 0.84 mm tip were tested at pressure of 2.5 bar and 5.0 bar.

4.3 Results and discussion

The results and discussion are separated into three categories: Electrical properties, Mechanical and electromechanical properties, and printability properties.

4.4 Electrical properties

The resistivity was measured after curing and after removing the samples from the mould, straining them, and letting them rest overnight. Table 4.2 shows the results. As expected, the resistivity values increased after removal. However, these values are still considerably lower than predicted using manufacturer data. This indicates an excellent dispersion for all formulations. The data was overlayed on the manufacturer's percolation graph in Figure 4.4. This shows that the results follow a similar trend to the manufacturer data. Comparing the results to other studies is difficult. Quinsaat et al. obtained ever lower resistivities using Ketjenblack EC-600JD but at much higher filler contents with 8.33 Ω cm at 12 wt% and 1.85 Ω cm at 22 wt% [91]. High filler content could be achieved likely due to the specialised formulation and the advanced processing steps taken. Most importantly this material was not 3D printed. Only one study showed both resistivity and 3D printing of two-dimensional structures. The resistivity using Ecoflex 00-30 / Vulcan XC72R was over three times higher at 5 wt% compared to what was found here [83].

Table 4.2: Resistivity measurements

Filler content (wt%)	Predicted resistivity (Ω cm)	Resistivity after cure (Ω cm)	Resistivity after removal (Ω cm)
3.5	725.86	68.79	169.09
4.0	353.90	38.01	80.31
4.5	184.83	23.29	49.13
5.0	105.81	16.41	36.00
5.5	67.12	9.89	22.33

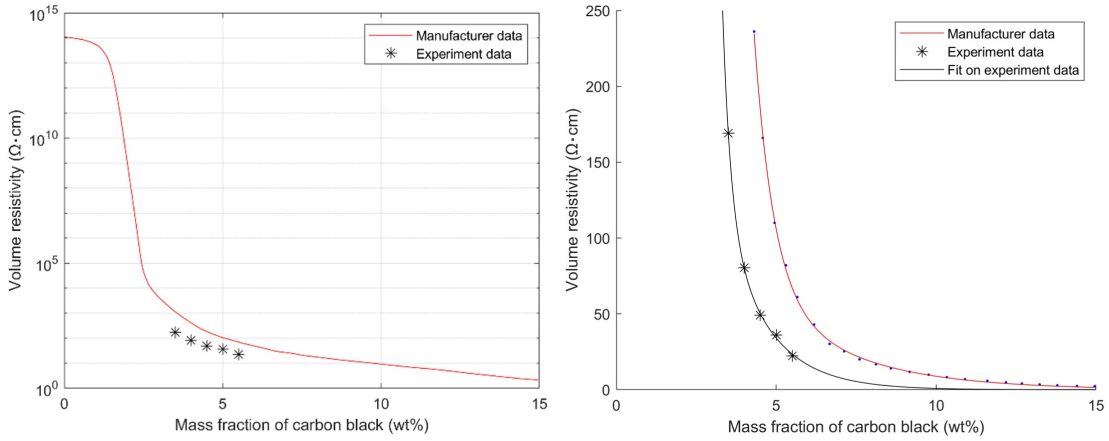

Figure 4.4: Resistivities found during the experiment and fit using a two-term exponential model.

4.5 Mechanical and electromechanical properties

When trying to load the samples into the test setup, it was found that the formulation with 5.5 % filler was too fragile for testing. The material appeared to be insufficiently cured. The remaining four formulations were thus tested: 3.5%, 4.0%, 4.5% and 5.0%. The results from test E1 for the lowest and highest filler content are shown in Figure 4.5. The material can function as a resistive strain sensor. These graphs already reveal that the 5.0% formulation has a larger mechanical hysteresis, the stress curve follows the position less accurately. The electrical response is better at the lower frequency due to the lower strain rate.

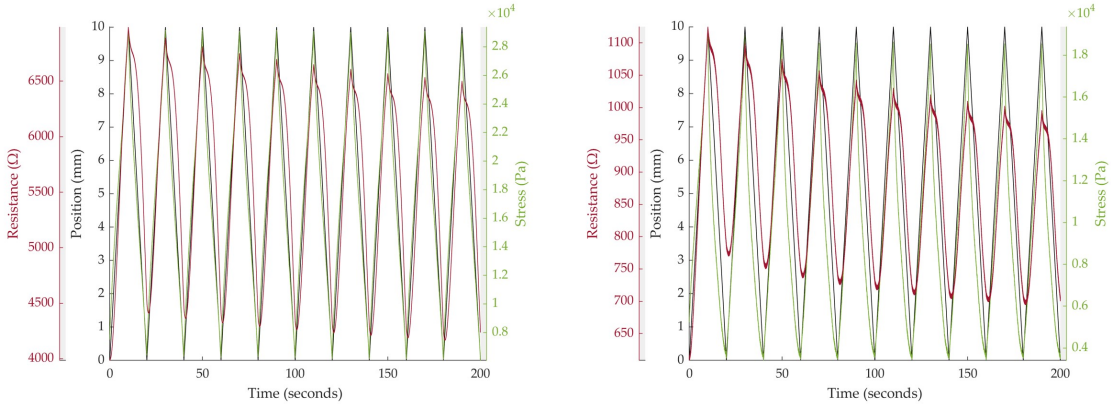

Figure 4.5: Test with 0.05 Hz triangle wave **(left)** 3.5 wt% **(right)** 5.0 wt%.

The mechanical behaviour is investigated further by plotting stress-strain curves of the conductive material in Figure 4.6. Both the results from E1 and E3 are shown here. Only data from the last period of each test is used to minimize transient effects. Young's modulus and hysteresis values calculated from this data are shown in Figure 4.7 and Figure 4.8. The Young's moduli are far below the maximum of 100 MPa determined in desired characteristic S1. Higher filler contents cause a decline in Young's modulus. This was also observed in literature [77]. The hysteresis is defined as the enclosed area of the last period. The mechanical hysteresis worsened considerably from the material without CB filler but did not have a clear relation to filler content. These factors do not affect the suitability of the material for soft robotic applications.

The structural material, Silopren LSR UV 2030, was tested in a similar manner. This material showed Young's moduli of 4.566×10^5 Pa in the 0.05 Hz test and 4.742×10^5 Pa in the 0.5 Hz test. This is approximately ten times that of Ecoflex 00-30 but still well within the range interesting

for soft robotic applications. The hysteresis values were 5329 J m^{-3} and 6482 J m^{-3} respectively. These are relatively high indicating more prominent viscous behaviour. To obtain a better understanding of the viscoelastic behaviour of these materials, a dynamic mechanical analysis could be performed using the data from E2 and E4 in the future.

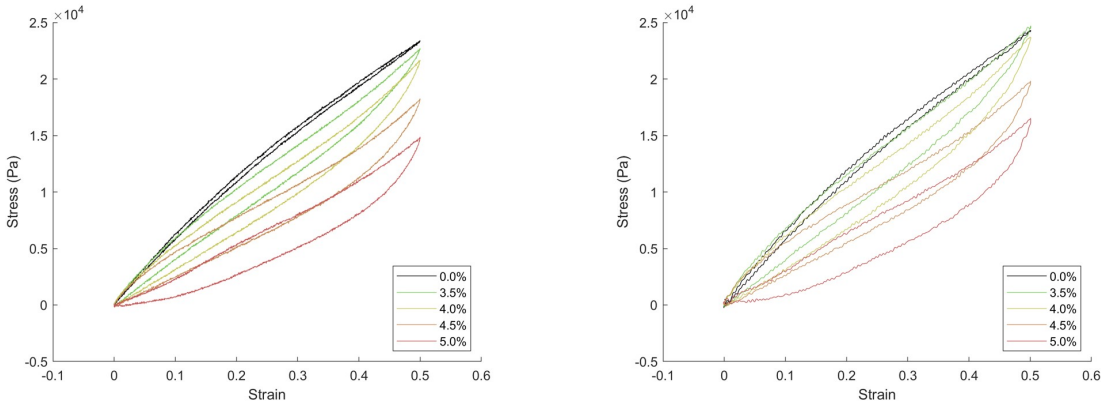

Figure 4.6: Stress-strain curves of the last period **(left)** 0.05 Hz **(right)** 0.5 Hz.

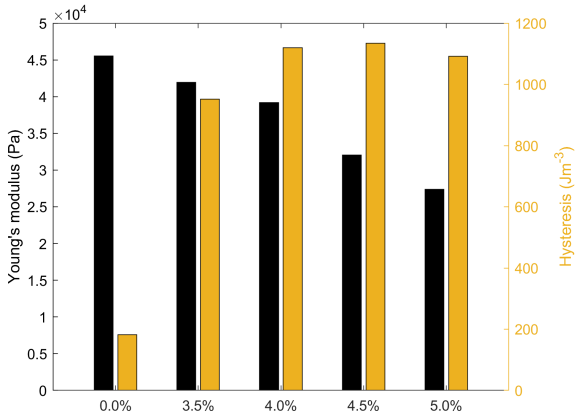

Figure 4.7: Young's moduli and hysteresis with 0.05 Hz triangle wave.

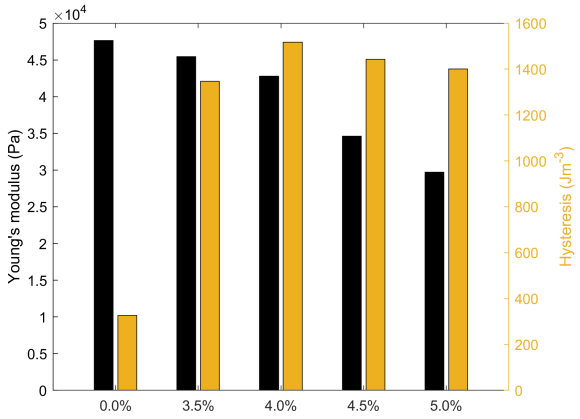

Figure 4.8: Young's moduli and hysteresis with 0.5 Hz triangle wave.

Electromechanical characterisation is important to assess the behaviour of the material as a sensor. Resistance-strain curves are shown in Figure 4.9. The results from E1 and E3 are shown here. Only data from the last period of each test is used to minimize transient effects. Gauge factor and hysteresis values calculated from this data are shown in Figure 4.10 and Figure 4.11.

The hysteresis defined here is the enclosed area of the last period. The geometric contribution to the gauge factor is close to 2. However, the results show gauge factors ranging from 0.91 to 1.14 for 0.05 Hz and from 0.73 to 0.91 for 0.5 Hz. This is lower than observed in relevant silicone / CB literature (see Table 2.3). Both gauge factor and hysteresis decrease with filler content. Literature has shown similar results [66, 77]. This behaviour can be explained using the percolation curve. The higher the filler content, the flatter the slope of the curve is. Changes in resistivity have a smaller contribution at higher filler content. Resistivity values with a higher slope on the percolation curve benefit the gauge factor but promote nonlinear behaviour which is reflected as hysteresis. Higher gauge factors should be possible with lower filler content than tested here. However, this will also increase hysteresis and the resistivity of the material.

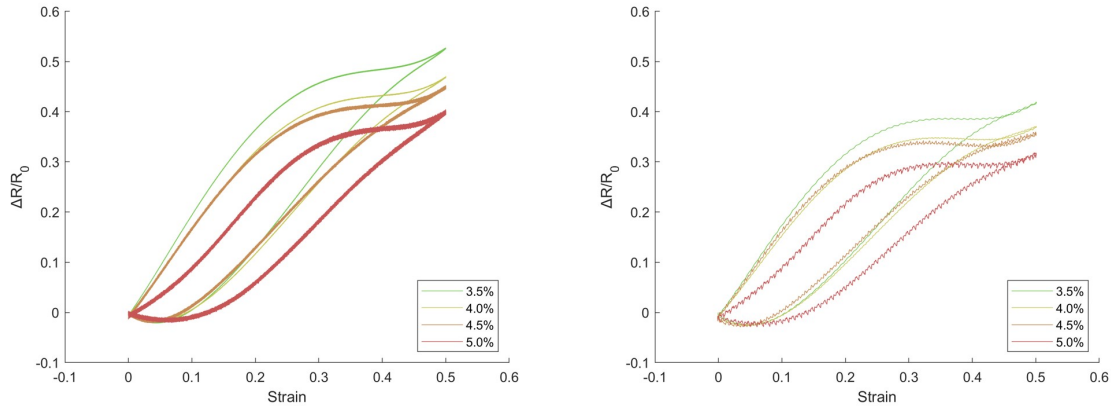

Figure 4.9: Resistance-strain curves of the last period **(left)** 0.05 Hz **(right)** 0.5 Hz.

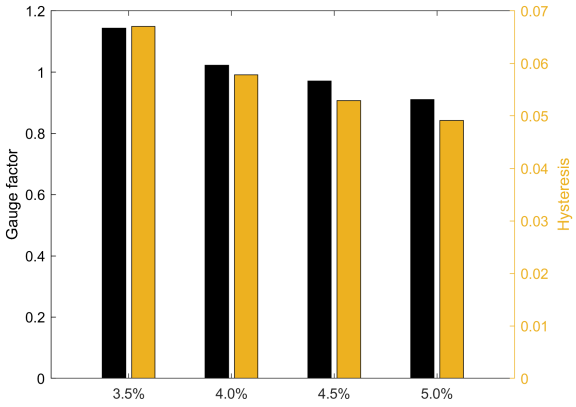

Figure 4.10: Gauge factor and hysteresis with 0.05 Hz triangle wave

No plastic deformation was observed during the aforementioned tests. The strain amplitude was increased from 50% to 200%. This resulted in plastic deformation of the sample with 5.0 wt% filler content as shown in figure 4.12. Higher filler content formulations have limited capability to survive high strains.

4.6 Printability properties

Extrusion of the materials was attempted. The larger 0.84 mm tip did not affect the printability of the materials. Formulations with 2.5 wt%, 3.0 wt% and 3.5 wt% could be extruded at 2500 mbar using both the 0.41 mm 0.84 mm tips. Formulations with 4.5 wt% and 5.0 wt% could only be extruded at 5000 mbar using both tips. The formulation with 5.5% failed to extrude at both nozzle sizes and pressures. The viscosity of this mixture was too high. The filler content limit for materials printable with the Pneuma Tool is thus 5.0 wt%.

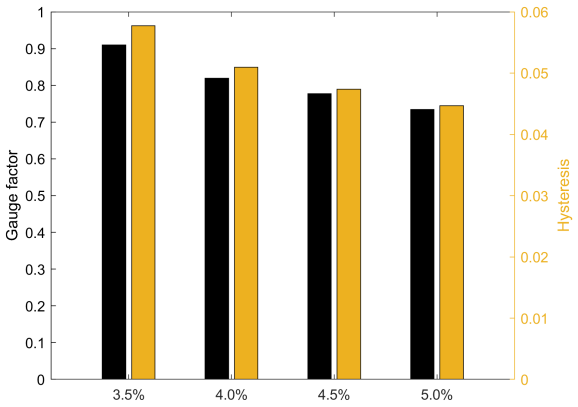

Figure 4.11: Gauge factor and hysteresis with 0.5 Hz triangle wave

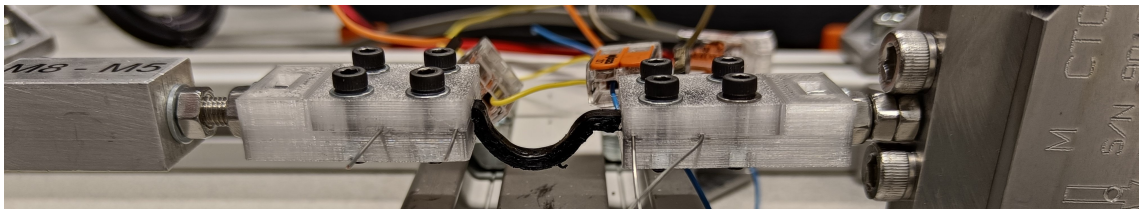

Figure 4.12: Plastic deformation occurred with the 5.0 wt% sample when strained to 200%

4.7 Conclusion

This chapter aimed to answer the following research sub-question: *"How does the formulation of the developed conductive material affect the mechanical, electrical, electromechanical and printability properties?"*. Ketjenblack EC-600JD was selected for the 3D printing process due to its excellent electrical properties and minimal effect on curing behaviour. Four formulations were tested: 3.5 wt%, 4.0 wt%, 4.5 wt%, 5.0 wt% and 5.5 wt%. The latter failed to cure within 20 hours and failed to extrude at a pressure of 5 bar. This formulation is unsuitable for the 3D printing process. The other formulations were analysed further. Better than predicted resistivities ranging from 36.00 Ω cm (5.0 wt%) to 169.09 Ω cm (3.5 wt%). Higher filler contents were shown to decrease resistivity, decrease Young's modulus, unclearly affect mechanical hysteresis, decrease gauge factor, decrease electrical hysteresis, and increase the pressure required for printing. The conductive material formulations show a Young's modulus of approximately a tenth of that of the structural material. Both exhibit excellent material properties for soft robotic applications. The found gauge factors between 0.73 and 1.14 were lower than expected. Higher gauge factors can be achieved with lower filler content than tested here. An overview of the material properties determined in this chapter is found in Table 4.3.

Table 4.3: List of material properties for tested materials

				Conductive				Structural
Property	Unit	0.0	3.5	4.0	4.5	5.0	5.5	0.0
Young's modulus at 0.05 Hz	kPa	45.54	41.20	39.18	32.04	27.40	-	456.6
Young's modulus at 0.5 Hz	kPa	47.64	45.45	42.81	34.63	29.71	-	474.2
Mechanical hysteresis loop area at 0.05 Hz	Jm^{-3}	182	951	1120	1350	1092	-	5329
Mechanical Hysteresis loop area at 0.5 Hz	Jm^{-3}	327	1348	1517	1442	1401	-	6482
Resistivity	Ω cm	-	169.09	80.31	49.13	36.00	22.33	-
Gauge factor at 0.05 Hz		-	0.91	0.82	0.78	0.73	-	-
Gauge factor at 0.5 Hz		-	1.14	1.02	0.97	0.91	-	-
Electrical hysteresis loop area at 0.05 Hz		-	0.0577	0.0510	0.0474	0.0447	-	-
Electrical Hysteresis loop area at 0.5 Hz		-	0.0670	0.0578	0.0529	0.0491	-	-
Printable at 2.5 bar		-	yes	yes	no	no	no	-
Printable at 5.0 bar		-	yes	yes	yes	yes	no	-

5 Additive manufacturing

5.1 Introduction

To validate that these selected materials are suitable for 3D printing, they must be tested on the Brinter One DIW printer. Practical experience with the Brinter One and the selected materials is discussed here.

5.2 3D printing of the structural material

Studies have shown that Silopren UV LSR 2030 is a viable option for silicone 3D printing. Holländer et al. used this material without rheology modifiers [59]. An external UV light was used for continuous irradiation of the material. The print was post-cured for 5 minutes. Fay et al. used a rheology modifier to improve printing fidelity [60]. Their method also uses constant irridiation of the deposited material. Brinter recommends using this material incombination with the Pneuma Tool Heated/ UV. Irradtion either continiously or per-layer is adviced. Different approaches to printing this material on the Pneuma Tool will be tested.

5.2.1 Methods

A UV protected syringe (Nordson EFD Optimum) in combination with a 0.25 mm tip (Nordson EFD Smoothflow tapered dispense tip) were inserted into the Pneuma Tool. The tips are suitable for UV-curable inks. A model was designed to test the capabilites of the printer (see Figure 5.1). It features an increasing overhang, a thin wall, and two structures to force move commands through air in a compact form factor that measures 0.65 mL. Three approaches were tested:

1. Continious irradiation with Pneuma Tool.
2. Layer-by-layer irradtiation with Pneuma Tool (120 s).
3. Layer-by-layer irradtiation with tool changer LED module (120 s).

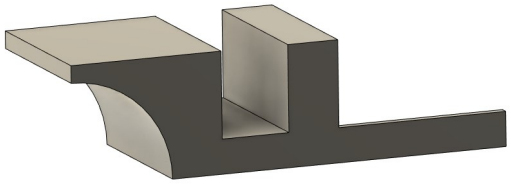

Figure 5.1: Model for testing the 3D printer

5.2.2 Results and discussion

Printing with the structural material was challenging. Obtaining reliable prints requires careful calibration of the flow by adjusting the pressure. A pressure of 2198 mbar was found to produce a correct flow for a print speed of 2 mm/s. Approach 1 left unsatisfactory results (see Figure 5.2). Continious exposure caused problem with imperfect extrusion. Silicone would easily accumulate near the tip, cure partically, and then spread across the print. The Pneuma Tool would also heat up from the LEDs. On one occasion, this caused the tip to crack as shown in Figure 5.3. Approach 2 failed to print the test model (see Figure 5.4). The tip would clog during the irradiation step after a few layers. Approach 3 yielded far superiour results (see Figure 5.5). The

seperation of the LED module allowed the tip to be unaffected by the curing steps. The downside of this approach is that the tool changer has to move to the position of the print after every layer. It is not possible to continuously irradiate the print with this LED module. Further testing is necessary to understand better means of protecting the tip from clogging. Transitioning to the Visco Tool will make printing with this material easier and more reliable.

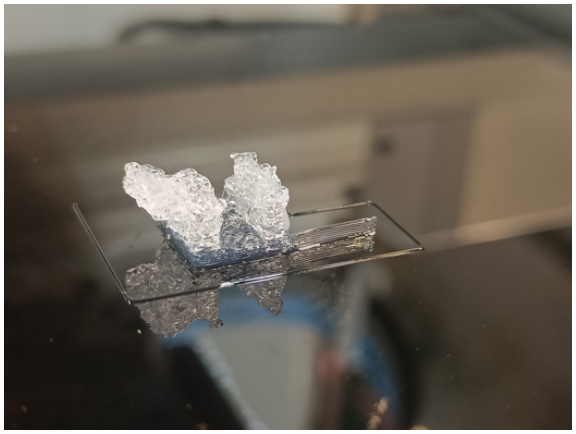

Figure 5.2: Test model 3D printed with approach 1

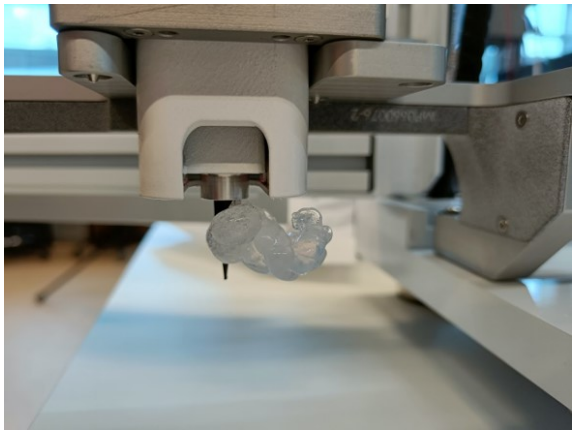

Figure 5.3: Failure under continuous exposure

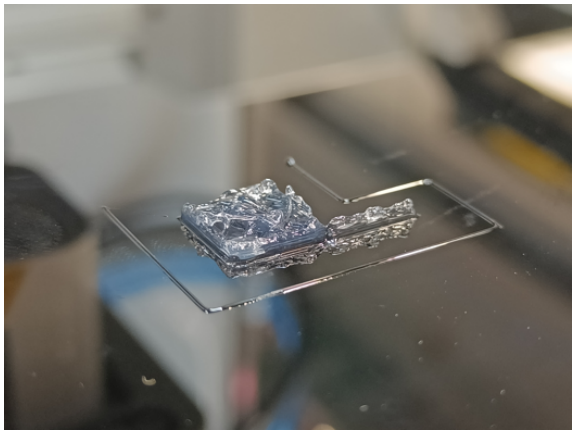

Figure 5.4: Test model 3D printed with approach 2

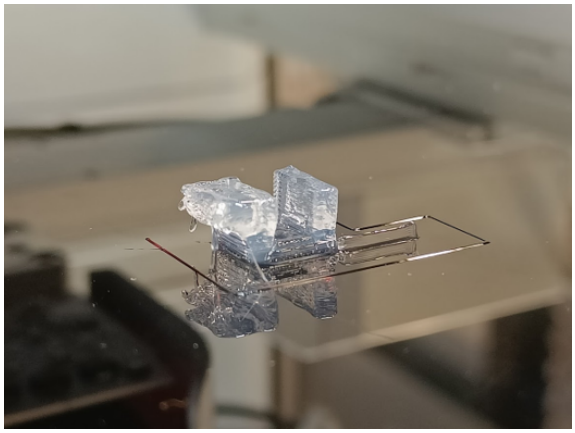

Figure 5.5: Test model 3D printed with approach 3

5.3 3D printing of the conductive material

Four suitable formulations of the conductive Ecoflex 00-30/ Ketjenblack EC-600JD were discussed. The goal of this experiment is to determine whether the lowest and highest filler content formulations can be 3D printed without rheology modifiers.

5.3.1 Methods

Formulations of 3.5 wt% and 5.0 wt% were synthesized using the procedure described in Table 3.5. A UV protected syringe (Nordson EFD Optimum) in combination with a 0.41 mm tip (Nordson EFD Smoothflow tapered dispense tip) were inserted into the Pneuma Tool. The print speed was set to 5 mm/s. The layer height to 0.41 mm. Five models were printed to test the print quality.

1. A cylinder with two walls, 20 mm tall: This will show if sagging occurs when printing.
2. The test model: To test the ability of the material to print overhangs and thin walls.
3. An octopus: To demonstrate that the material is capable of producing complex 3D printed shapes.

5.3.2 Results and discussion

Both materials printed excellently without rheological modifiers. No difference in printing quality was observed. The 3.5 wt% formualtion required a pressure of 2256 mbar while the 5.0 wt% formulation required a pressure of 4464 mbar. The 3.5 wt% started curing prematurely after approximately 3 hours. Results for the cilinder model are shown in Figure 5.6 and Figure 5.7. The cylinder was accidentally differently scaled for both materials. The height of the cylinder model for the 3.5 wt% sample was set to 15 mm while that for the 5.0 wt% sample was set to 20 mm. The height of both cylinders were exactly as designed, even after the oven cure. Results for the test model are shown in Figure 5.6 and Figure 5.8. Both formulations failed the overhang test halfway through the print. Printing of a thin wall did not give problems. The printed octopi are shown in Figure 5.9. Both materials were able to produce a high quality prints.

5.4 Conclusion

3D printing of Silopren UV LSR is challinging due to problems with material accumulation and clogging of the tip. The best approach was to cure the print using an LED module installed on the tool changer. More research is required to improve the quality of the prints. Both 3.5 wt% and 5.0 wt% formulations of the Ecoflex 00-30 / Ketjenblack EC-600JD compsoite were

printed succesfully. The materials show excellent shape retention without the need of rheological modiefiers.

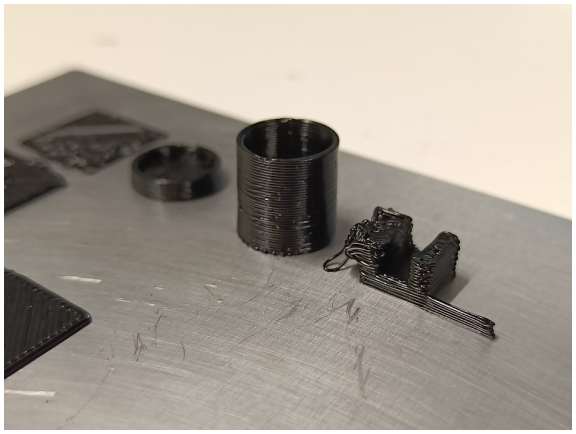

Figure 5.6: 3D printed cylinder model and test model printed with 3.5 wt% formulation

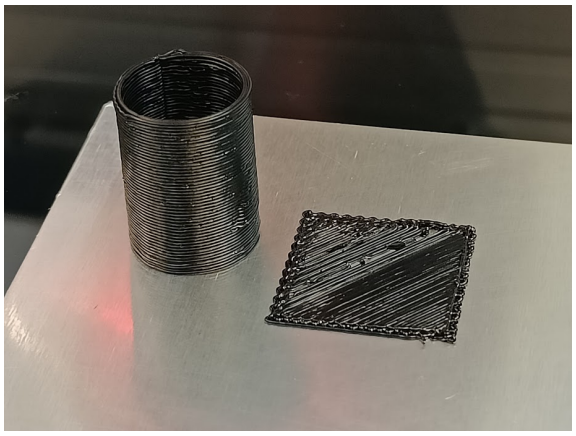

Figure 5.7: 3D printed cylinder model printed with 5.0 wt% formulation

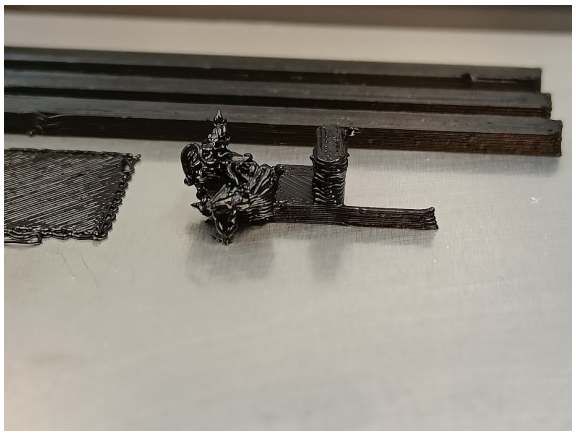

Figure 5.8: 3D printed test model printed with 5.0 wt% formulation

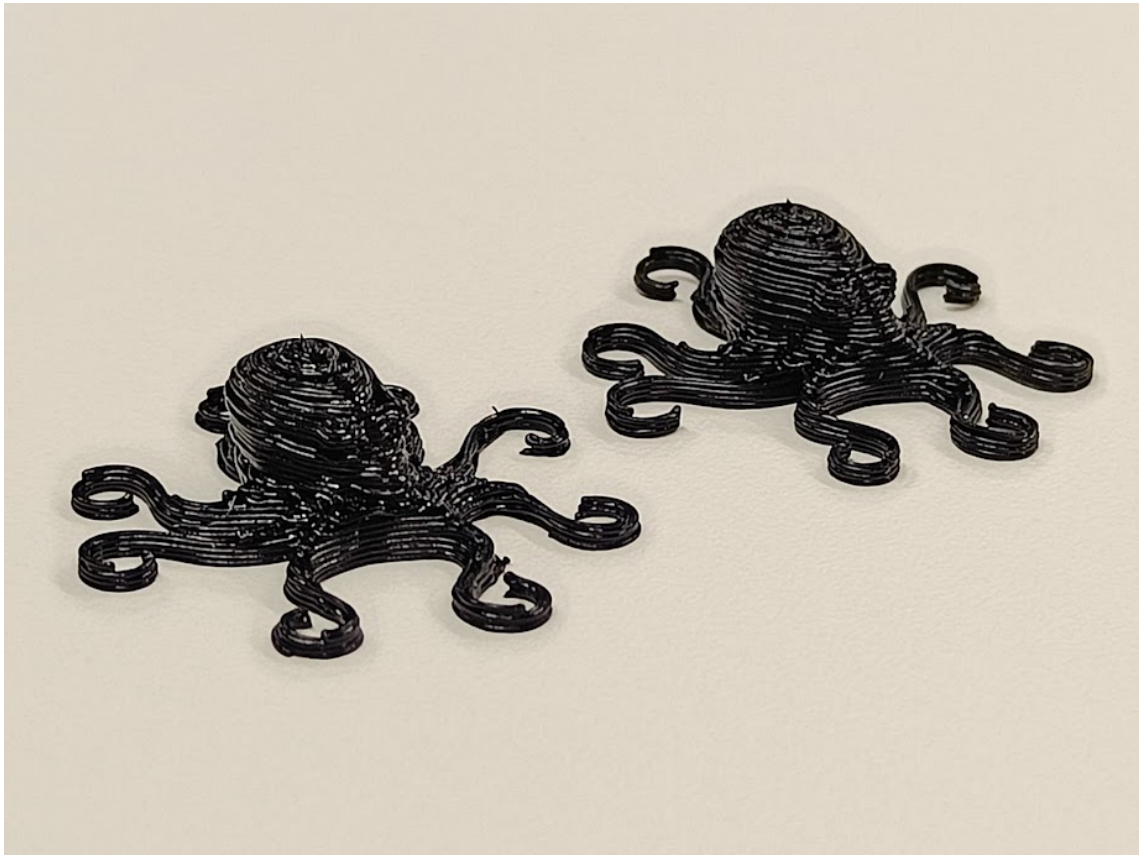

Figure 5.9: 3D printed octipi (**left**) 3.5 wt% (**right**) 5.0 wt%

6 Conclusions and Recommendations

6.1 Conclusions

Soft robots are inherently safe, adaptive, and tolerant to operating in unknown environments due to the sole use of soft materials. Recently, there has been a notable interest in enhancing the performance and enabling the autonomy of soft robots through the addition of sensing capabilities. Moreover, the use of 3D printing is gaining attention as a valuable approach for fabricating complex soft robots. Recent studies aiming to integrate these two developments have inadequately considered all aspects. The research question of this thesis was therefore:

> *What should a 3D printing process, that enables embedded sensing for soft robotic applications, look like?*

To support this research question, three research sub-questions were formulated relating to the selection of materials, method of processing, and characterisation of said materials.

> *Which structural and conductive materials comply with the demanding criteria of soft robotics while being compatible with the used DIW 3D printer?*

Silicone type materials were chosen to be the structural material as they exhibit favourable characteristics associated with soft robotic applications while being commercially available and requiring minimal processing complexity. A UV cure silicone, Silopren UV LSR 2030, was determined to be the most suitable structural material due to its excellent properties and unique ability to quickly cure on demand. Conductive silicone composite type materials were chosen as the conductive material as they are unique in their ability to facilitate complex self-supporting sensing structures both in embedded form and at the surface. From the considered conductive fillers, electroconductive carbon blacks (CB) were deemed best suited due to their accessibility, good processability and favourable rheological properties for 3D printing. Two filler types were selected, the industry-standard Vulcan XC72 and the electrical grade Ketjenblack EC-600JD. Ecoflex 00-30 was selected as the silicone matrix due to its excellent mechanical properties and low viscosity enabling the use of higher filler contents without additives.

> *How can the selected materials be processed successfully using a method with minimal complexity?*

Current literature on 3D printing of conductive silicone / CB composites insufficiently addresses methods of processing these materials. During this thesis, a reproducible and accessible procedure for processing these materials without the need for solvents was developed. The method uses a planetary centrifugal mixer to enable the synthesis of low and high viscosity mixtures with minimal effect on pot life. The method takes advantage of the accelerated cure behaviour exhibited by the additive system silicones by subjecting the materials to a temperature of 80 °C during the curing process. The exclusive use of mixing was insufficient to break down the palleted/beaded form of the fillers into agglomerates. The solution was found by grinding the CB filler into powder using zirconia pearls before mixing. Experiments on the grinding and mixing process revealed that mixtures with good dispersion and resistivity could be achieved at higher mixing speeds. Attempts to synthesize and cure materials with a predicted resistivity of 100 Ω cm showed that mixtures with Vulcan XC72 could not cure. Mixtures using Ketjenblack EC-600JD exhibited reduced impact on the curing process due to the lower required filler content and showed resistivity values that were a fifth of those seen with Vulcan XC72. The reached resistivity values surpassed manufacturer expectations and the high filler content formulation was printable, indicating a good quality of dispersion was achieved.

How does the formulation of the developed conductive material affect the mechanical, electrical, electromechanical and printability properties?

Current studies on soft robots with embedded sensors insufficiently characterise the properties of the sensor materials. This study tested the electrical, mechanical, electromechanical and printability properties of the Ecoflex 00-30 / Ketjenblack EC-600JD composite with formulations of 3.5 wt%, 4.0 wt%, 4.5 wt%, 5.0 wt% and 5.5 wt%. The 5.5 wt% formulation was determined unsuitable for the 3D printing process as it failed to cure within 20 hours and failed to extrude at a pressure of 5 bar. The other formualtions showed better than expected resistivities ranging from 36.00 Ω cm (5.0 wt%) to 169.09 Ω cm (3.5 wt%). An increase in filler content was shown to decrease resistivity, decrease Young's modulus, unclearly affect mechanical hysteresis, decrease gauge factor, decrease electrical hysteresis, and increase the pressure required for printing. The found gauge factors between 0.73 and 1.14 were lower than expected which reduces its use for applications that require high sensitivity. Higher gauge factors are expected to be achievable with much lower filler contents than tested, at the expense of higher electrical hysteresis.

Both the structural and the conductive material were shown to exhibit excellent properties for soft robotic applications and were printable using the Brinter One. In conclusion, an accessable 3D printing process that enables embedded sensing for soft robotic applications has been developed. The findings of this research offer a promising outlook, paving the way for further development of this 3D printing process.

6.1.1 Recommendations

The objective of this thesis was the selection, processing and characterisation of suitable materials. The 3D printing process has great potential for use in complex soft robots with embedded sensors. Further development of the 3D printing process is necessary to achieve this goal. Recommendations for further development are categorized in additive manufacturing and materials

Additive manufacturing

Initial tests were performed to verify the printability of the materials using the Brinter One. More experience with printing these materials using the Tools of the Brinter One is necessary to improve the printing quality and reliability. Support materials could be researched in order to improve design freedom. Most importantly, the structural and conductive material should be implemented by multi-material printing in order to print soft robots and soft sensors. This is expected to be a challenge on its own.

Materials

The structural material was printed successfully without rheology modifiers. However, its rheological behaviour could inflict bad shape retention when applying layer-by-layer curing on longer-duration prints. Rheology modifiers could be included to improve printing fidelity [60]. The conductive material showed excellent electrical, mechanical, electromechanical and printability properties. Higher filler content was found to interfere with the curing process. The use of hydrogen silicone oil to improve cure speed and degree of crosslinking as described by Dou et al. should be studied to enable the use of even higher filler content [82]. Lower filler content should be tested for sensing applications requiring higher gauge factors. Low filler content formulation may not exhibit suitable rheological properties for 3D printing and may cause premature curing during mixing. Additives such as rheology modifiers and cure retardants should be studied to enable low filler content formulations. The suitability of the materials for capacitive strain sensing should be studied to promote sensor designs with improved hysteresis and linearity.

A MoSCoW Prioritization

A.1 Required TexLive packages

Printing soft sensors using a novel method requires a multidisciplinary approach. A large number of experiments are to be performed due to this project's applied nature. These are experiments on material analysis, (multi-material) 3D printing, and sensing. Each of these topics could be explored to such an extent that they cover multiple theses. The challenge is thus to select a realistic research plan in which the goal of creating a 3D printing process can be met while maintaining adequate academic research value. The aim of this chapter is to create an overview of the project with the current state of knowledge. A prioritization of the tasks to cover in this thesis is made using the MoSCoW method.

A.2 Project overview and task prioritization

Potential tasks to be performed in this project are divided into three categories: materials, additive manufacturing, and soft actuators with embedded sensors. A prioritization of these tasks is made using the MoSCoW method. The prioritization classes are defined as follows.

- Must: Tasks necessary for successful completion of the thesis.
- Should: Tasks important for a good result but not necessary.
- Could: Tasks that are nice to include but have a smaller impact.
- Won't: Tasks that are not a priority within this thesis' timeframe but might be interesting in future research.

A.2.1 Materials

1. Structural material
    1.1. Literature study: What is the state of research regarding 3D printing silicones (for soft robotics)? How are conventional silicones and UV curing silicones applied?
    1.2. Material selection: What are desired properties? Which products are suitable for the 3D printing of soft robots?
    1.3. Processing: What processing steps are necessary to prepare the silicone for 3D printing?
    1.4. Analysis
        1.4.1. Uncured material
            1.4.1.1. Mixed viscosity: What is the viscosity of the silicone after adding the necessary ingredients? Does the material show shear thinning/thickening behaviour?
            1.4.1.2. Pot life: How does the viscosity change over time under lab conditions? How does this affect the 3D printing process?
        1.4.2. Curing characteristics
            1.4.2.1. Photopolymerization kinetics model: How can the curing of UV silicones be modelled?
            1.4.2.2. UV-curing time How can the degree of curing of silicone be determined using experiments? How does layer thickness influence curing? How do the duration and strength of the light source affect curing?

1.4.3. Mechanical testing

1.4.3.1. Hardness testing: What is the shore durometer of the cured material?

1.4.3.2. Elasticity testing: What is the value of the relevant elastic modulus? How can this be tested?

1.4.3.3. Tensile testing: What are the tensile strength, yield strength and elongation at break?

1.4.3.4. Dynamic mechanical analysis: What are the viscoelastic properties?

2. Conductive material

2.1. Literature study: Which types conductive materials are used in (3D printed) soft sensor research?

2.2. Material selection: What are the desired properties? Which type of material is best suited for 3D printing of sensors in soft robots? Which products are suitable?

2.3. Processing: What processing steps are necessary to prepare the material for 3D printing? How do the mixing parameters affect the conductivity of the uncured material?

2.4. Analysis

2.4.1. Uncured material

2.4.1.1. Mixed viscosity: How is the viscosity affected by the filler content? Does the material show shear thinning behaviour?

2.4.1.2. Pot life: How does the viscosity change over time under lab conditions? How is this affected by filler content? How does this affect the 3D printing process?

2.4.1.3. Printability: How does the filler contnet affect printability? This means 1) the achievable print speed under pressure and 2) the ability to hold its extruded shape.

2.4.2. Curing characteristics: How is curing affected by filler content? How can the curing be delayed or accelerated?

2.4.3. Resistivity: How does the filler content affect the resistivity of the material?

2.4.4. Mechanical testing

2.4.4.1. Hardness testing: How is the shore durometer affected by filler content?

2.4.4.2. Elasticity testing: What is the value of the relevant elastic modulus? How is this affected by filler content?

2.4.4.3. Tensile testing: What are the tensile strength, yield strength and elongation at break? How are they affected by filler content?

2.4.4.4. Dynamic mechanical analysis: What are the viscoelastic properties? How are they affected by content?

2.4.4.5. Resistance under strain: How does the resistance of the test sample behave under strain? How are the hysteresis/nonlinearities and the gauge factor affected by filler content?

2.4.5. Composition selection: What range of filler content is suitable for 3D printing of soft robotic sensors given the results from the experiments?

3. Material interaction

3.1. Curing: Is the curing of one material affected by another?

3.2. Adhesion: What is the adhesive strength of the materials?

A.2.2 Additive manifacturing

1. Literature study: What are considerations related to the (multi-material) 3D printing of silicone (sensors) found in literature?
2. 3D printing of structural material: Which method is successful at printing the structural material?
3. 3D printing of conductive material: Which method is successful at printing the conductive material?
4. Multi-material 3D printing: Which method is successful at printing the materials together?
5. Comparison to bulk material samples: How do printed samples compare to bulk material in the mechanical and electrical tests?

A.2.3 Soft actuators with embedded sensors

1. Literature study: What were the results of similar studies?
2. Actuator design: Develop a soft actuator with embedded strain sensor.
3. Actuator/sensor model: How can the actuator and sensor be modelled?
4. Actuator fabrication: What is the total process of producing the actuator?
5. Actuator/sensor characterisation: How does the sensor behave? How do the results differ from the model?

A.3 Motivation

The overview clearly shows the extent of this project. A total of 37 tasks have been listed. While all interesting, the priority with respect to this thesis varies among these tasks. Motivation for the selection of tasks to be addressed in this thesis is in order.

The overview shows a substantial amount of work within the research of materials. This is a vital component of the project but it should be explored with caution. Material science quickly becomes overly complex and time-consuming, especially due to my lack of experience in this field on an academic level. It is easy to lose oneself in its various aspects. The choice was made to focus on the conductive material within the materials category. High-priority tasks for the structural material are limited to selection, processing, and a single mechanical test. The other mechanical tests have a weaker contribution while requiring far more time and effort. Understanding and modelling the curing characteristics of this material would be valuable but was determined to require advanced knowledge of material science. The time required to obtain this knowledge is better spent on tasks of higher impact as this task would only yield a reduction in printing duration. Experiments on the uncured material have little value as the viscosity should be known by the manufacturer of the structural material. Research on the conductive material is of greater importance. The main purpose of the research on this material is to find suitable compositions. The effect of the filler content on the electrical, electromechanical, and printability properties should be studied with various experiments. Additional mechanical tests and a study on the curing characteristics are considered of lower priority for comparable reasons to the functional material. Following the characterisation of the materials, methods of applying these in an additive manufacturing process must be developed. This concerns the individual materials as well as the combination of these materials in a multi-material process. Only the former is considered realistic in the timeframe of this thesis. A multi-material printing approach and its application by fabricating a soft actuator with embedded sensors are to be included in future studies.

Bibliography

[1] G. Alici, "Softer is harder: What differentiates soft robotics from hard robotics?," in *MRS Advances*, vol. 3, pp. 1557–1568, Materials Research Society, 2018.

[2] J. Shintake, V. Cacucciolo, D. Floreano, and H. Shea, "Soft Robotic Grippers," *Advanced Materials*, vol. 30, 7 2018.

[3] R. F. Shepherd, F. Ilievski, W. Choi, S. A. Morin, A. A. Stokes, A. D. Mazzeo, X. Chen, M. Wang, and G. M. Whitesides, "Multigait soft robot," *PNAS*, vol. 108, no. 51, pp. 20400–20403, 2011.

[4] F. Ahmed, M. Waqas, B. Jawed, A. M. Soomro, S. Kumar, A. Hina, U. Khan, K. H. Kim, and K. H. Choi, "Decade of bio-inspired soft robots: A review," *Smart Materials and Structures*, vol. 31, 7 2022.

[5] H. Wang, M. Totaro, and L. Beccai, "Toward Perceptive Soft Robots: Progress and Challenges," *Advanced Science*, vol. 5, 9 2018.

[6] T. J. Wallin, J. Pikul, and R. F. Shepherd, "3D printing of soft robotic systems," *Nature Reviews Materials*, vol. 3, pp. 84–100, 6 2018.

[7] Y. Zhou and H. Li, "A Scientometric Review of Soft Robotics: Intellectual Structures and Emerging Trends Analysis (2010–2021)," *Frontiers in Robotics and AI*, vol. 9, 5 2022.

[8] E. Sachyani Keneth, A. Kamyshny, M. Totaro, L. Beccai, and S. Magdassi, "3D Printing Materials for Soft Robotics," *Advanced Materials*, vol. 33, no. 19, p. 2003387, 2020.

[9] Brinter, "Brinter ONE – Multitool 3D bioprinter."

[10] Deltatower GmbH, "Delta Tower Fluid ST."

[11] Lynxter, "S600D Universal 3D Printer,"

[12] N. El-Atab, R. B. Mishra, F. Al-Modaf, L. Joharji, A. A. Alsharif, H. Alamoudi, M. Diaz, N. Qaiser, and M. M. Hussain, "Soft Actuators for Soft Robotic Applications: A Review," *Advanced Intelligent Systems*, vol. 2, p. 2000128, 10 2020.

[13] F. Ilievski, A. D. Mazzeo, R. F. Shepherd, X. Chen, and G. M. Whitesides, "Soft robotics for chemists," *Angewandte Chemie - International Edition*, vol. 50, pp. 1890–1895, 2 2011.

[14] B. Mosadegh, P. Polygerinos, C. Keplinger, S. Wennstedt, R. F. Shepherd, U. Gupta, J. Shim, K. Bertoldi, C. J. Walsh, and G. M. Whitesides, "Pneumatic networks for soft robotics that actuate rapidly," *Advanced Functional Materials*, vol. 24, pp. 2163–2170, 4 2014.

[15] G. Stano, L. Arleo, and G. Percoco, "Additive manufacturing for soft robotics: Design and fabrication of airtight, monolithic bending PneuNets with embedded air connectors," *Micromachines*, vol. 11, 5 2020.

[16] H. K. Yap, H. Y. Ng, and C. H. Yeow, "High-Force Soft Printable Pneumatics for Soft Robotic Applications," *Soft Robotics*, vol. 3, pp. 144–158, 9 2016.

[17] H. M. C. M. Anver, R. Mutlu, and G. Alici, "3D Printing of a Thin-Wall Soft and Monolithic Gripper Using Fused Filament Fabrication," in *IEEE International Conference on Advanced Intelligent Mechatronics (AIM)*, pp. 442–447, 2017.

[18] R. B. Scharff, E. L. Doubrovski, W. A. Poelman, P. P. Jonker, C. C. Wang, and J. M. Geraedts, "Towards behavior design of a 3D-printed soft robotic hand," *Biosystems and Biorobotics*, vol. 17, pp. 23–29, 2017.

[19] D. Wang, C. Jiang, J. Wang, and L. Dong, "Soft Actuators and Robots Enabled by Additive Manufacturing," *Annual Review of Control, Robotics, and Autonomous Systems*, vol. 6, 5 2023.

[20] S. Coyle, C. Majidi, P. Leduc, and K. J. Hsia, "Bio-inspired Soft Robotics: Material Selection, Actuation, and Design," tech. rep., 2018.

[21] S. C. Shit and P. Shah, "A review on silicone rubber," *National Academy Science Letters*, vol. 36, pp. 355–365, 8 2013.

[22] M. Wehner, R. L. Truby, D. J. Fitzgerald, B. Mosadegh, G. M. Whitesides, J. A. Lewis, and R. J. Wood, "An integrated design and fabrication strategy for entirely soft, autonomous robots," *Nature*, vol. 536, pp. 451–455, 8 2016.

[23] R. L. Truby, M. Wehner, A. K. Grosskopf, D. M. Vogt, S. G. M Uzel, R. J. Wood, and J. A. Lewis, "Soft Somatosensitive Actuators via Embedded 3D Printing," *Advanced Materials*, vol. 30, p. 1706383, 4 2018.

[24] R. L. Truby, R. K. Katzschmann, J. A. Lewis, and D. Rus, "Soft Robotic Fingers with Embedded Ionogel Sensors and Discrete Actuation Modes for Somatosensitive Manipulation; Soft Robotic Fingers with Embedded Ionogel Sensors and Discrete Actuation Modes for Somatosensitive Manipulation," in *2019 2nd IEEE International Conference on Soft Robotics (RoboSoft)*, 2019.

[25] O. Dogan Yirmibesoglu, J. Morrow, S. Walker, W. Gosrich, R. Canizares, H. Kim, U. Daalkhaijav, C. Fleming, C. Branyan, and Y. Menguc, *Direct 3D printing of silicone elastomer soft robots and their performance comparison with molded counterparts*. 2018.

[26] J. Li, S. Wu, W. Zhang, K. Ma, and G. Jin, "3D Printing of Silicone Elastomers for Soft Actuators," *Actuators*, vol. 11, 7 2022.

[27] M. Manns, J. Morales, and P. Frohn, "Additive manufacturing of silicon based PneuNets as soft robotic actuators," in *Procedia CIRP*, vol. 72, pp. 328–333, Elsevier B.V., 2018.

[28] H. Banerjee, M. Suhail, and H. Ren, "Hydrogel actuators and sensors for biomedical soft robots: Brief overview with impending challenges," 9 2018.

[29] J. Odent, T. J. Wallin, W. Pan, K. Kruemplestaedter, R. F. Shepherd, and E. P. Giannelis, "Highly Elastic, Transparent, and Conductive 3D-Printed Ionic Composite Hydrogels," *Advanced Functional Materials*, vol. 27, 9 2017.

[30] W. Sun, S. Schaffer, K. Dai, L. Yao, A. Feinberg, and V. Webster-Wood, "3D Printing Hydrogel-Based Soft and Biohybrid Actuators: A Mini-Review on Fabrication Techniques, Applications, and Challenges," 4 2021.

[31] Y. Cheng, K. Hoe Chan, X.-Q. Wang, T. Ding, T. Li, X. Lu, and G. Wei Ho, "Direct-Ink-Write 3D Printing of Hydrogels into Biomimetic Soft Robots," 2019.

[32] S. Li, H. Zhao, and R. F. Shepherd, "Flexible and stretchable sensors for fluidic elastomer actuated soft robots," *MRS Bulletin*, vol. 42, pp. 138–142, 2 2017.

[33] M. Elwenspoek, G. Krijnen, and R. Wiegerink, *Introduction to Mechanics and Transducer Science*. University of Twente, 2008.

[34] M. Schouten, G. Wolterink, A. Dijkshoorn, D. Kosmas, S. Stramigioli, and G. Krijnen, "A Review of Extrusion-Based 3D Printing for the Fabrication of Electro-and Biomechanical Sensors," *Special issue on 20 years IEEE sensors journal*, 2020.

[35] D. Kosmas, M. Schouten, and G. Krijnen, "Hysteresis Compensation of 3D Printed Sensors by a Power Law Model with Reduced Parameters," in *FLEPS 2020 - IEEE International Conference on Flexible and Printable Sensors and Systems*, Institute of Electrical and Electronics Engineers Inc., 8 2020.

[36] T. Helps and J. Rossiter, "Proprioceptive Flexible Fluidic Actuators Using Conductive Working Fluids," *Soft Robotics*, vol. 5, pp. 175–189, 4 2018.

[37] T. Kim, D. M. Kim, B. J. Lee, and J. Lee, "Soft and deformable sensors based on liquid metals," *Sensors (Switzerland)*, vol. 19, 10 2019.

[38] G. D. Goh, G. L. Goh, Z. Lyu, M. Z. Ariffin, W. Y. Yeong, G. Z. Lum, D. Campolo, B. S. Han, and H. Y. A. Wong, "3D Printing of Robotic Soft Grippers: Toward Smart Actuation and Sensing," 11 2022.

[39] H. W. Tan, J. An, C. K. Chua, and T. Tran, "Metallic Nanoparticle Inks for 3D Printing of Electronics," *Advanced Electronic Materials*, vol. 5, 5 2019.

[40] N. Ibrahim, J. O. Akindoyo, and M. Mariatti, "Recent development in silver-based ink for flexible electronics," *Journal of Science: Advanced Materials and Devices*, vol. 7, 3 2022.

[41] A. Koivikko, E. S. Raei, M. Mosallaei, M. Mäntysalo, and V. Sariola, "Screen-printed curvature sensors for soft robots," *IEEE Sensors Journal*, vol. 18, pp. 223–230, 1 2018.

[42] S. Kim, J. Oh, D. Jeong, W. Park, and J. Bae, "Consistent and Reproducible Direct Ink Writing of Eutectic Gallium-Indium for High-Quality Soft Sensors," *Soft Robotics*, vol. 5, pp. 601–612, 10 2018.

[43] H. Devaraj, T. Giffney, A. Petit, M. Assadian, and K. Aw, "The development of highly flexible stretch sensors for a Robotic Hand," *Robotics*, vol. 7, 9 2018.

[44] T. Calais, N. D. Sanandiya, S. Jain, E. V. Kanhere, S. Kumar, R. Chen-Hua Yeow, and P. Valdivia Alvarado, "Freeform Liquid 3D Printing of Soft Functional Components for Soft Robotics," *ACS Appl. Mater. Interfaces*, vol. 14, 2022.

[45] S. S. Robinson, K. W. O'Brien, H. Zhao, B. N. Peele, C. M. Larson, B. C. Mac Murray, I. M. Van Meerbeek, S. N. Dunham, and R. F. Shepherd, "Integrated soft sensors and elastomeric actuators for tactile machines with kinesthetic sense," *Extreme Mechanics Letters*, vol. 5, pp. 47–53, 12 2015.

[46] B. Shih, C. Christianson, K. Gillespie, S. Lee, J. Mayeda, Z. Huo, and M. T. Tolley, "Design considerations for 3D printed, soft, multimaterial resistive sensors for soft robotics," *Frontiers Robotics AI*, vol. 6, no. APR, p. 30, 2019.

[47] R. L. Truby and J. A. Lewis, "Printing soft matter in three dimensions," *Nature*, vol. 540, pp. 371–378, 12 2016.

[48] Y. Li and B. Li, "Direct ink writing 3D printing of polydimethylsiloxane-based soft and composite materials: A mini review," *Oxford Open Materials Science*, vol. 2, no. 1, 2022.

[49] A. V. Radchenko and F. Ganachaud, "Photocatalyzed Hydrosilylation in Silicone Chemistry," *Industrial and Engineering Chemistry Research*, vol. 61, pp. 7679–7698, 6 2022.

[50] Jayven Yeo, Junqiang Justin Koh, Fuke Wang, Zibiao Li, and Chaobin He, "3D Printing Silicone Materials and Devices," in *Silicon Containing Hybrid Copolymers*, pp. 239–263, 2020.

[51] E. J. Courtial, C. Perrinet, A. Colly, D. Mariot, J. M. Frances, R. Fulchiron, and C. Marquette, "Silicone rheological behavior modification for 3D printing: Evaluation of yield stress impact on printed object properties," *Additive Manufacturing*, vol. 28, pp. 50–57, 8 2019.

[52] L. Y. Zhou, Q. Gao, J. Z. Fu, Q. Y. Chen, J. P. Zhu, Y. Sun, and Y. He, "Multimaterial 3D Printing of Highly Stretchable Silicone Elastomers," *ACS Applied Materials and Interfaces*, vol. 11, pp. 23573–23583, 7 2019.

[53] S. Gharaie, A. Zolfagharian, A. A. A. Moghadam, N. Shukur, M. Bodaghi, B. Mosadegh, and A. Kouzani, "Direct 3D printing of a two-part silicone resin to fabricate highly stretchable structures," *Progress in Additive Manufacturing*, 2023.

[54] J. Chen, J. Liu, Y. Yao, and S. Chen, "Effect of microstructural damage on the mechanical properties of silica nanoparticle-reinforced silicone rubber composites," *Engineering Fracture Mechanics*, vol. 235, 8 2020.

[55] Elkem, "Additive Manufacturing / 3D Printing with AMSil™ Silicones."

[56] L. Jaksa, D. Pahr, G. Kronreif, and A. Lorenz, "Development of a Multi-Material 3D Printer for Functional Anatomic Models," *International Journal of Bioprinting*, vol. 7, no. 4, pp. 145–155, 2021.

[57] L. Jaksa, D. Pahr, G. Kronreif, and A. Lorenz, "Calibration Dependencies and Accuracy Assessment of a Silicone Rubber 3D Printer," *Inventions*, vol. 7, 6 2022.

[58] E.-J. Courtial, A. Colly, and C. A. Marquette, "Dynamic Molding Deposition: The additive manufacturing in partially ordered system," *Additive Manufacturing*, vol. 51, p. 102598, 2022.

[59] J. Holländer, R. Hakala, J. Suominen, N. Moritz, J. Yliruusi, and N. Sandler, "3D printed UV light cured polydimethylsiloxane devices for drug delivery," *International Journal of Pharmaceutics*, vol. 544, pp. 433–442, 6 2018.

[60] C. D. Fay, A. Jeiranikhameneh, S. Sayyar, S. Talebian, A. Nagle, K. Cheng, S. Fleming, P. Mukherjee, and G. G. Wallace, "Development of a customised 3D printer as a potential tool for direct printing of patient-specific facial prosthesis," *International Journal of Advanced Manufacturing Technology*, vol. 120, pp. 7143–7155, 6 2022.

[61] A. Saleem, L. Frormann, and A. Soever, "Fabrication of extrinsically conductive silicone rubbers with high elasticity and analysis of their mechanical and electrical characteristics," *Polymers*, vol. 2, pp. 200–210, 9 2010.

[62] P. J. Brigandi, J. M. Cogen, and R. A. Pearson, "Electrically conductive multiphase polymer blend carbon-based composites," *Polymer Engineering and Science*, vol. 54, pp. 1–16, 1 2014.

[63] Y. Zheng, X. Huang, J. Chen, K. Wu, J. Wang, and X. Zhang, "A review of conductive carbon materials for 3d printing: Materials, technologies, properties, and applications," *Materials*, vol. 14, 7 2021.

[64] M. Tavakoli, R. Rocha, L. Osorio, M. Almeida, A. De Almeida, V. Ramachandran, A. Tabatabai, T. Lu, and C. Majidi, "Carbon doped PDMS: Conductance stability over time and implications for additive manufacturing of stretchable electronics," *Journal of Micromechanics and Microengineering*, vol. 27, 2 2017.

[65] V. Kumar, M. N. Alam, A. Manikkavel, M. Song, D. J. Lee, and S. S. Park, "Silicone rubber composites reinforced by carbon nanofillers and their hybrids for various applications: A review," *Polymers*, vol. 13, 7 2021.

[66] J. Shintake, E. Piskarev, S. H. Jeong, and D. Floreano, "Ultrastretchable Strain Sensors Using Carbon Black-Filled Elastomer Composites and Comparison of Capacitive Versus Resistive Sensors," *Advanced Materials Technologies*, vol. 3, 3 2018.

[67] E. R. Cholleti, J. Stringer, M. Assadian, V. Battmann, C. Bowen, and K. Aw, "Highly Stretchable Capacitive Sensor with Printed Carbon Black Electrodes on Barium Titanate Elastomer Composite," *Sensors (Basel, Switzerland)*, vol. 19, no. 1, 2019.

[68] H. Lian, M. Xue, K. Ma, D. Mo, L. Wang, Z. Cui, and X. Chen, "Three-Dimensional Printed Carbon Black/PDMS Composite Flexible Strain Sensor for Human Motion Monitoring," *Micromachines*, vol. 13, p. 1247, 8 2022.

[69] H. T. Deng, D. L. Wen, T. Feng, Y. L. Wang, X. R. Zhang, P. Huang, and X. S. Zhang, "Silicone Rubber Based-Conductive Composites for Stretchable "all-in-One" Microsystems," *ACS Applied Materials and Interfaces*, vol. 14, pp. 39681–39700, 9 2022.

[70] Y. Zhu, M. Assadian, M. Ramezani, and K. C. Aw, "Printing of Soft Stretch Sensor from Carbon Black Composites," *MDPI Proceedings*, p. 732, 12 2018.

[71] A. S. Kurian, T. Giffney, J. Lee, J. Travas-Sejdic, and K. C. Aw, "Printing of CNT/silicone rubber for a wearable flexible stretch sensor," in *Electroactive Polymer Actuators and Devices (EAPAD) 2016*, vol. 9798, p. 97980K, SPIE, 4 2016.

[72] C. Fekiri, H. C. Kim, and I. H. Lee, "3d-printable carbon nanotubes-based composite for flexible piezoresistive sensors," *Materials*, vol. 13, pp. 1–12, 12 2020.

[73] H. Devaraj, R. Schober, M. Picard, M. Y. Teo, C. Y. Lo, W. C. Gan, and K. C. Aw, "Highly elastic and flexible multi-layered carbon black/elastomer composite based capacitive sensor arrays for soft robotics," *Measurement: Sensors*, vol. 2-4, p. 100004, 8 2019.

[74] J. Yuan, Y. Zhang, G. Li, S. Liu, and R. Zhu, "Printable and Stretchable Conductive Elastomers for Monitoring Dynamic Strain with High Fidelity," *Advanced Functional Materials*, vol. 32, 8 2022.

[75] I. S. Yoon, Y. Oh, S. H. Kim, J. Choi, Y. Hwang, C. H. Park, and B. K. Ju, "3D Printing of Self-Wiring Conductive Ink with High Stretchability and Stackability for Customized Wearable Devices," *Advanced Materials Technologies*, vol. 4, 9 2019.

[76] Easy Composites, "ADDITION CURE SILICONE RUBBER," tech. rep.

[77] W. Yi, Y. Wang, G. Wang, and X. Tao, "Investigation of carbon black/silicone elastomer/dimethylsilicone oil composites for flexible strain sensors," *Polymer Testing*, vol. 31, pp. 677–684, 8 2012.

[78] Momentive, "Silicone Elastomers," tech. rep., 2018.

[79] Smooth-On, "Durometer Shore Hardness Scale."

[80] P. Seppälä, "Carbon black magic turning electrically conductive plastics into products," *https://blog.premixgroup.com/carbon-black-magic-turning-electricall-conductive-plastics*, 2021.

[81] Birla Carbon, "Carbon Black 101," *https://www.birlacarbon.com/whats-trending/carbon-black/*.

[82] Y. Dou, S. Sun, S. Lu, W. Yao, and D. Guan, "Preparation of carbon black/silicone rubber composites with large-area-homogeneous-low electrical-resistance used as electroplating matrix," *RSC Advances*, vol. 12, pp. 32448–32458, 11 2022.

[83] H. Devaraj, K. Yellapantula, M. Stratta, A. McDaid, and K. Aw, "Embedded piezoresistive pressure sensitive pillars from piezoresistive carbon black composites towards a soft large-strain compressive load sensor," *Sensors and Actuators, A: Physical*, vol. 285, pp. 645–651, 1 2019.

[84] K. Yellapantula, H. Devaraj, M. Assadian, L. Stuart, C. Y. Lo, W. C. Gan, and K. Aw, "Soft and flexible sensor array using carbon black pillars for object recognition via pressure mapping," *Measurement: Journal of the International Measurement Confederation*, vol. 159, 7 2020.

[85] S. Yong and K. Aw, "Multi-Layered Carbon-Black/Elastomer-Composite-Based Shielded Stretchable Capacitive Sensors for the Underactuated Robotic Hand," *Robotics*, vol. 11, 6 2022.

[86] L. A. Garcia-Garcia, G. Valsamakis, P. Kreitmair, N. Munzenrieder, and D. Roggen, "Inferring Complex Textile Shape from an Integrated Carbon Black-infused Ecoflex-based Bend and Stretch Sensor Array," in *Adjunct Proceedings of the 2021 ACM International Joint Conference on Pervasive and Ubiquitous Computing and Proceedings of the 2021 ACM International Symposium on Wearable Computers*, pp. 298–303, Association for Computing Machinery, Inc, 9 2021.

[87] M. R. Binelli, R. van Dommelen, Y. Nagel, J. Kim, R. I. Haque, F. B. Coulter, G. Siqueira, A. R. Studart, and D. Briand, "Digital manufacturing of personalised footwear with embedded sensors," *Scientific Reports*, vol. 13, 12 2023.

[88] M. Eklund and N. Kjäll, *Silicone-based Carbon Black Composite for Epidermal Electrodes*. PhD thesis, 2019.

[89] Y. Xia, Q. Zhang, X. E. Wu, T. V. Kirk, and X. D. Chen, "Practical and durable flexible strain sensors based on conductive carbon black and silicone blends for large scale motion monitoring applications," *Sensors (Switzerland)*, vol. 19, 10 2019.

[90] F. M. Yaul, V. Bulovic, and J. H. Lang, "A flexible underwater pressure sensor array using a conductive elastomer strain gauge," in *Proceedings of the IEEE International Conference on Micro Electro Mechanical Systems (MEMS)*, pp. 500–503, 2012.

[91] J. E. Q. Quinsaat, I. Burda, R. Krämer, D. Häfliger, F. A. Nüesch, M. Dascalu, and D. M. Opris, "Conductive silicone elastomers electrodes processable by screen printing," *Scientific Reports*, vol. 9, 12 2019.

[92] S. Rosset, O. A. Ararom, S. Schlatter, and H. R. Shea, "Fabrication process of silicone-based dielectric elastomer actuators," *Journal of Visualized Experiments*, vol. 2016, 2 2016.

[93] S. Geraedts, *Pore Size Distribution and Surface Group Analysis A study of two electrical grade carbon blacks*. PhD thesis, 2002.

[94] Productive Innovations, "DAC SpeedMill," *https://www.productiveinnovations.co.uk/speedmill*.